International Geology Review, Vol. 42, 2000, p. 865–894.

The Solar System's Earliest Chemistry: Systematics of Refractory Inclusions

TREVOR R. IRELAND[1]

Department of Geological and Environmental Sciences, Stanford University, California 94305-2115

AND BRUCE FEGLEY, JR.

Planetary Chemistry Laboratory, Deptartment of Earth and Planetary Sciences, Washington University, St. Louis, Missouri 63130

I was going to church with Graeme, he was only a little fellow then, and I heard a rumbling noise. I looked up and saw smoke and wondered what the dickens it was.

— Mr. Reg Orr, Murchison, Australia

Abstract

Refractory inclusions, or CAIs (calcium-aluminium–rich inclusions) are a unique ingredient in chondritic meteorites. As the name suggests, they are enriched in refractory elements, essentially reflecting a condensation sequence of phases from a cooling gas of solar composition. However, the widespread preservation of diverse isotopic anomalies is not compatible with the inclusions having been in a gaseous form. Rather, the CAIs appear to represent mixtures of condensate and refractory residue materials. The condensates formed from cooling solar gas and fractionation of that gas produced variations in the abundances of refractory elements according to volatility. Solar condensate has isotopically normal Ca and Ti isotopic compositions and has $^{26}Al/^{27}Al$ of the canonical value for the solar system at 5×10^{-5}. Residues of material falling in toward the Sun are probably aluminous oxides such as corundum and hibonite, and preserve diverse Ca and Ti isotopic anomalies. Meteoritic inclusions from the Murchison meteorite show the best polarization of these components. Spinel-hibonite-perovskite inclusions (SHIBs) predominantly have normal Ca and Ti isotopes, $^{26}Al/^{27}Al$ at 5×10^{-5}, and ultrarefractory fractionated REE patterns. Single hibonite crystal fragments (PLACs) have diverse Ca and Ti isotopic compositions and low $^{26}Al/^{27}Al$ because of the initially high proportion of ^{27}Al in the residue. REE patterns in PLACs are variable in terms of the ultrarefractory fractionation of their REE patterns, as indicated by Tm/Tm*, but are dominated by depletion in the less refractory REE Eu and Yb. Both PLACs and SHIBs homogenized with ^{16}O-rich gas, enriched relative to terrestrial O by up to 7%, thus removing any isotopic heterogeneity from the PLAC precursors. CAIs formed close to the Sun where condensation and re-evaporation of REE was possible, and were then ejected back to planetary radii where they were eventually accreted onto planetesimals.

Introduction

THE STUDY OF ISOTOPIC ANOMALIES in meteorites has forged ahead in recent years with the discovery of interstellar grains that probably formed as direct condensates around other stars (Zinner, 1998). Almost lost in the rapidly exploding data set are refractory inclusions or CAIs (calcium-aluminium–rich inclusions), which have played a pivotal role in concepts of solar system formation. CAIs are rich in refractory elements and attest to high-temperature processes in the solar nebula (Grossman, 1980). They are viewed as the most primitive materials produced in the solar system because they have the oldest Pb/Pb ages of any objects at ~4.566 Ga (Allègre et al., 1995) and they have excess ^{26}Mg, from decay of the short-lived radionuclide ^{26}Al with an initial $^{26}Al/^{27}Al$ ratio of 5×10^{-5} (Lee et al., 1977), which is far higher than any other type of solar-system object. Furthermore, CAIs contain ubiquitous isotopic anomalies in elements such as O, Ca, and Ti; their preservation suggests formation prior to

[1]Current address: Research School of Earth Sciences, The Australian National University, Canberra, ACT 0200, Australia.

0020-6814/00/483/865-30 $10.00

homogenization of source materials in the solar system. While CAIs are not direct stellar condensates, the size of some of the CAI isotopic anomalies rivals those in interstellar grains, suggesting minimal processing between stellar condensation and crystallization into their present form in the solar system.

CAIs are a common component of carbonaceous chondrites but it was not until 1969 that researchers were presented with an abundance of these objects (Marvin et al., 1970). Two large carbonaceous chondrites fell in that year: in Mexico, the Allende CV3 chondrite fell with a recovered weight of approximately 2000 kg (Clark et al., 1970); and in Australia, the Murchison CM2 chondrite fell with a recovered weight of approximately 100 kg (Fuchs et al., 1973). Inclusions from both of these meteorites were set upon with state-of-the-art analytical equipment designed for analysis of the lunar return samples. However, despite extensive study over the past 30 years, their origins remain enigmatic. Their original interpretation as condensates from the solar nebula (Marvin et al., 1970; Grossman, 1972) was based on the compatibility of CAI mineralogy with the sequence of phases predicted to condense from a cooling gas of solar composition, and mineralogical textures such as fluffy aggregates of microscopic crystals that appear to be direct gas-solid condensates. Furthermore, Allende CAIs are typically enriched in refractory trace elements by about a factor of 20 with respect to chondritic abundances, suggesting that they could represent the first 5% of condensed rock-forming elements. Such an origin was also consistent with the non-detection (at that time) of isotopic anomalies in the lithophile elements because in the gas phase, isotopic anomalies are quickly homogenized leading to the average solar isotopic abundances.

The condensation model was so simple and appealing that even with the discovery of ubiquitous (and diverse) isotopic anomalies in elements such as O and Ti, the concept of local gas reservoirs with distinct compositions was advanced. In this case, local heterogeneities are maintained in the solar system in the gas phase, and the precipitation of distinct CAIs reflected the local gas composition. However, in detail, the systematics of these inclusions suggest that their formation is a more complicated process. In part, the systematics have been determined by high-temperature processing, but it is likely that relict solid material was involved as well, and the inclusions may have been through more than one heating cycle after their initial formation.

This paper reviews the characteristics of CAIs and attempts to place them in a framework for their formation in the solar system. The main source of CAIs has been the Allende and Murchison meteorites. Other meteorites have some distinctive characteristics in their CAIs, but in some ways, every CAI is unique, and there is no point in examining the unique aspects of every inclusion if an overall picture of CAI formation is to be obtained. The CAIs from Allende and Murchison basically contain the full range of CAIs known, and so discussion will be limited to the major characteristics of CAIs from each of these meteorites.

The literature is rich in chemical and isotopic data from many CAIs (e.g., Clayton and Davis, 1988), but there has been only limited success in the interpretation of what these characteristics are telling us. Thus a major goal of this paper is to place a limited number of chemical and isotopic characteristics of CAIs in an internally consistent framework. The characteristics chosen are the major isotopic and chemical features that set CAIs apart from other inclusions in chondrites. The features include the refractory nature of CAIs, the volatility fractionations in the REE patterns, and isotopic abundances of magnesium, titanium, and oxygen.

Refractory Inclusions

CAIs from the Allende CV3 chondrite

Grossman (1975) petrographically divided Allende CAIs into two main types (A and B), each of which had two subgroups—"fluffy" and "compact." Type A CAIs were composed predominantly of melilite with less spinel, whereas Type B CAIs have pyroxene as the dominant mineral with melilite, spinel, and plagioclase. However, the compositional limits proposed by Grossman (1975) appear to be rather restrictive, as noted by Mason and Taylor (1982) who analyzed a suite of inclusions for trace elements. Essentially Types A and B might be more appropriately considered as endmembers of the compositional range. Fluffy CAIs appear to have the characteristics of condensates, being friable assemblages of small crystals, whereas the compact CAIs are more consistent with a molten origin. However, such a distinction cannot be uniquely determined, and the petrographic distinctions between condensate, melt, and xenocrystic material cannot be made with great confidence.

What can be readily seen is that the mineralogy of the Allende CAIs is consistent with the phases

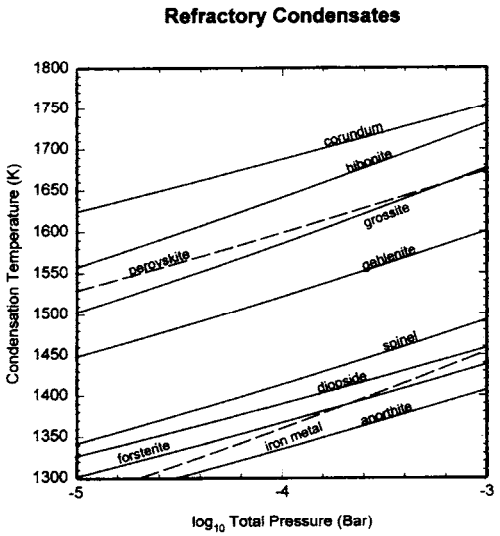

FIG. 1. Condensation temperatures as a function of total nebular pressure for refractory minerals found in CAIs and several lower-temperature phases. Modified from Lodders and Fegley (1993) and Lauretta and Lodders (1997). The different phases shown are stable on and below the labeled lines.

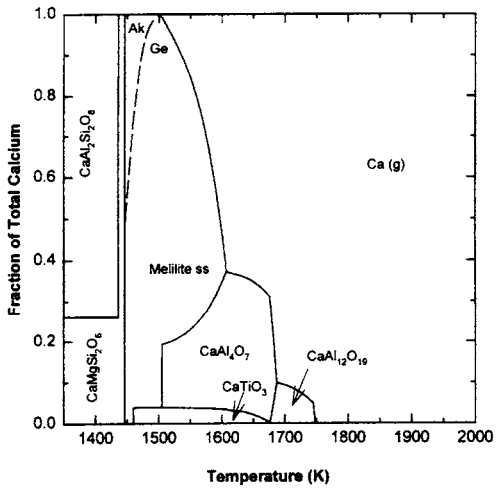

FIG. 2. Equilibrium chemistry of calcium in the solar nebula at 10^{-3} bar total pressure. The dominant gas is monatomic Ca, which condenses into different Ca-bearing minerals with decreasing temperature. The first condensate is hibonite ($CaA_{12}O_{19}$), followed by grossite ($CaAl_4O_7$) and perovskite ($CaTiO_3$). Most of the Ca gas is eventually consumed by formation of melilite solid solution. The dashed line shows the amounts of gehlenite and åkermanite in melilite. Calcium is 50% condensed at 1615 K and is distributed between Ca-bearing clinopyroxene (represented by diopside) and plagioclase (represented by anorthite) at low temperatures. Modified from Lauretta and Lodders (1997).

predicted to condense from a cooling gas of solar composition at pressures of 10^{-5} to 10^{-3} bar (Grossman, 1972). As illustrated in Figure 1, the first phases to condense from a solar-composition gas should be refractory oxides such as corundum (Al_2O_3), calcium aluminates (hibonite [$CaAl_{12}O_{19}$] and grossite [$CaAl_4O_7$]), and perovskite ($CaTiO_3$). With decreasing temperature, these phases back-react with nebular gas to form other less refractory oxides and aluminosilicates. For example, Figures 2 and 3 show that Ca aluminates react with nebular gas to form melilite. Initially the melilite is almost pure gehlenite ($Ca_2Al_2SiO_7$), but as temperatures continue to decrease, increasing proportions of åkermanite ($Ca_2MgSi_2O_7$) become incorporated into the melilite. Further decreases in temperature lead to formation of spinel ($MgAl_2O_4$), clinopyroxenes (represented in Figure 1 by diopside [$CaMgSi_2O_6$]), plagioclase feldspar (represented in Figure 1 by anorthite [$CaAl_2Si_2O_8$]), forsterite (Mg_2SiO_4), and Fe metal alloy. The mineral sequence is somewhat dependent upon the total nebular pressure (e.g., see the intersecting grossite and perovskite lines or the forsterite and iron metal lines in Figure 1), and the details of the gas-solid reactions as a function of temperature are somewhat complex (Figs. 2 and 3).

However, the overall picture that emerges is that the Allende CAI mineralogy represents the middle to lower range of temperatures, because both the highest-temperature phases (e.g., corundum, hibonite, and grossite) and the lower-temperature phases (anorthite, forsterite, and Fe metal alloy) are generally absent. It appears that the most refractory oxides have back-reacted with nebular gas to form less refractory phases such as melilite, pyroxene, spinel, and plagioclase, and that most Allende CAIs were chemically isolated from nebular gas prior to condensation of Fe alloy and significant amounts of anorthite and forsterite.

The high-temperature origin of the mineralogy is also consistent with the trace-element systematics of CAIs. A common attribute for CAIs is a light-rare-earth-element (LREE) abundance of ~10–20 times chondritic levels. If the CAIs were produced during the condensation of a gas of solar composition, then this enrichment can be interpreted as all of the REE being condensed into only a few phases, and to get a 20-fold enrichment, only 5%

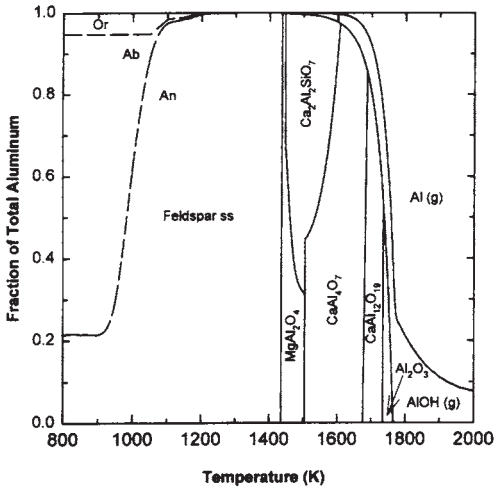

FIG. 3. Equilibrium chemistry of aluminum in the solar nebula at 10^{-3} bar total pressure. The dominant gases are monatomic Al and AlOH, which initially condense into corundum. Hibonite and other Al-bearing condensates form with decreasing temperature. Aluminum is 50% condensed at 1735 K and is distributed between orthoclase (or), albite (ab), and anorthite (an) at lower temperatures. Modified from Lauretta and Lodders (1997).

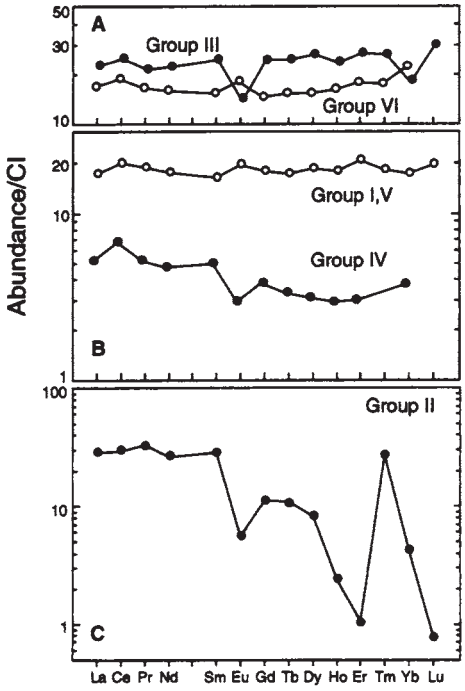

FIG. 4. REE abundance patterns most commonly found in Allende refractory inclusions. Mason and Taylor (1982) divided the patterns into six groups. The CAIs typically have LREE abundances of ~10–20 x chondritic levels. Group I has a relatively unfractionated pattern with only a small positive Eu anomaly, Group II has a highly fractionated pattern with much lower abundances of the heavy REE Gd-Er and Lu, Group III has negative anomalies of Eu and Yb, Group IV are olivine-rich inclusions that have a relatively unfractionated pattern at 2–4 x chondrite levels, Group V is unfractionated, and Group VI has small positive anomalies at Eu and Yb.

of the rocky material (e.g., Mg, Si, Fe, Ca, Al, Ti, etc.) would have condensed. Mason and Taylor (1982) described six discrete groups of patterns that represent some subtle, and some not so subtle, variations from flat chondritic abundances (Fig. 4). Group I has a relatively unfractionated pattern with only a small positive Eu anomaly, Group II has a highly fractionated pattern with much lower abundances of the heavy-rare-earth-element (HREE) Gd-Er and Lu, Group III has negative anomalies of Eu and Yb, Group IV has a relatively unfractionated pattern at 2–4 times chondrite levels, Group V is unfractionated, and Group VI has small positive anomalies at Eu and Yb (Figs. 4A–4C).

Only a loose correspondence with texture was noted: Groups I, V, and VI are predominantly melilite-rich chondrules, Groups II and III are mainly fine-grained aggregates, and Group IV is composed of olivine-rich aggregates and chondrules. Fegley and Ireland (1991) noted that there is a significant potential bias in the relative abundances of these patterns in Allende CAIs. The easiest CAIs to obtain from Allende are the largest inclusions, which range in size up to 2 cm. These inclusions have predominantly Group I, V patterns. Smaller CAIs have Groups II and III patterns more commonly.

REE patterns in CAIs can be described as the result of three different processes, two of which are related to volatility, and the other resulting from magmatic partitioning. The volatility effects are illustrated in Figure 5 for Allende CAIs from three main groups, with the elements reordered into a relative volatility sequence. For the Group I, V pattern in Figure 5A, both the REE pattern and volatility pattern show near-flat chondrite-normalized patterns at approximately 20 times CI. The most volatile element V does appear to show a slight relative depletion, being only ~10 times CI. In Figure 5B, Group III patterns are shown for Ca-rich and Ca-poor CAI compositions after Kornacki and Fegley

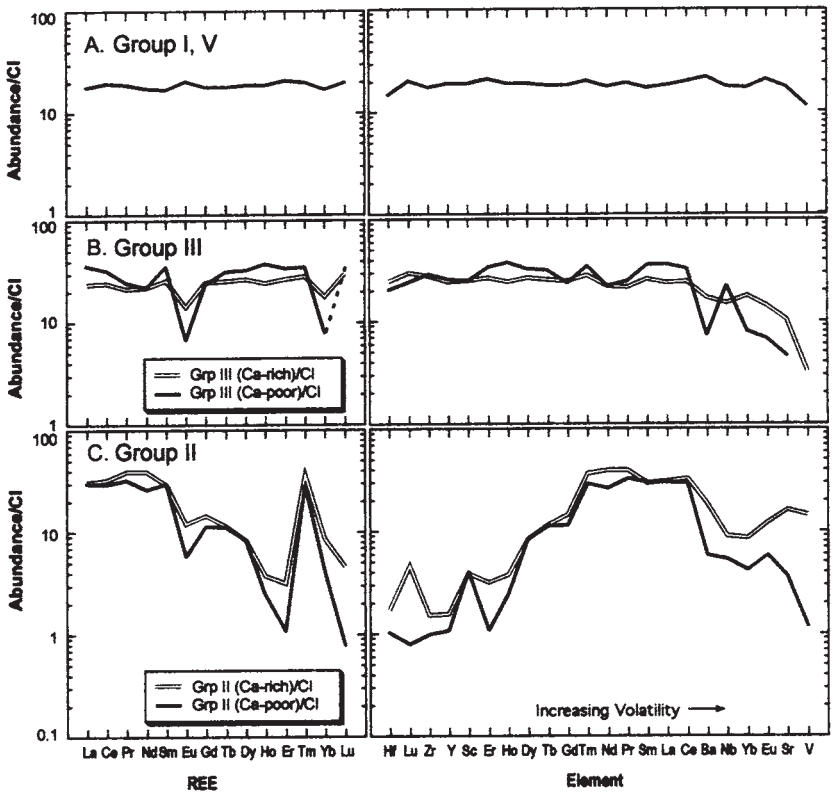

FIG. 5. The most common REE patterns are shown on the left, and trace-element patterns in order of increasing volatility (or decreasing condensation temperature) are shown on the right. The Group I,V pattern is relatively unfractionated in REE as well as the other refractory lithophile elements shown. Group III patterns show Eu and Yb anomalies, which are the most volatile of the REE, and this is consistent with the trace-element pattern, which shows a progressive depletion in the more volatile elements with unfractionated more-refractory elements. Group II inclusions show depletions in the most volatile and the most refractory elements. Data from Kornacki and Fegley (1986) subdivided into Ca-rich and Ca-poor inclusions for Groups II and III.

(1986). Eu and Yb are the most volatile REE, and these elements, along with the other relatively volatile elements Ba, Nb, Sr, and V are depleted. The Ca-rich CAIs exhibit a very smooth progressive depletion, whereas the Ca-poor inclusions are somewhat more scattered. In Figure 5C, the Group II pattern is seen to be depleted in the most refractory, as well as the most volatile elements, while the light REE and Tm are present in similar abundances to Group I, V and III patterns.

The depletions in the most volatile elements in the Group III pattern can be produced either by condensation, in which case the condensate must have been isolated from the gas prior to condensation of the more volatile elements, or by distillation, whereby a CAI with a chondritic pattern, albeit elevated in overall abundance, is raised in temperature until the more volatile elements are evaporated. The Group II pattern, which is depleted in the most refractory and the most volatile REE, is apparently consistent only with a condensation origin. Obtaining that pattern requires removal of the most ultrarefractory elements, either in an earlier condensate that is then isolated from the remaining gas, or left behind as a residue (Boynton, 1975). CAIs with ultrarefractory-enriched patterns have not been found in Allende, but were first found in Murchison (Boynton et al., 1980), and will be described below.

Thus the different REE patterns observed in CAIs are predominantly the result of volatility-controlled fractionations rather than igneous partitioning. The latter pattern, shown for a terrestrial basalt

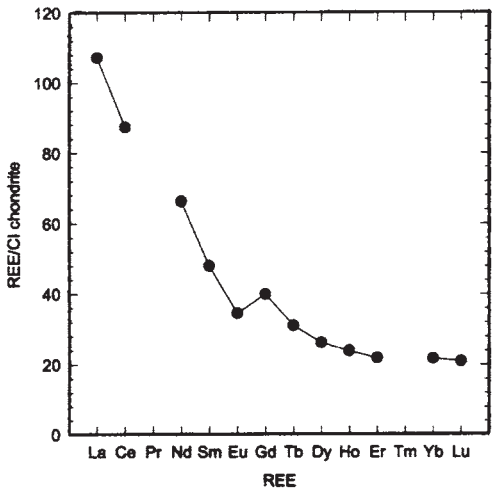

FIG. 6. REE abundance pattern in a terrestrial basalt (BCR-1) from Haskin et al. (1971). Analytical values for Pr or Tm do not exist because these elements are difficult to measure in terrestrial samples by neutron activation analysis.

in Figure 6, has a characteristic Eu depletion caused by the incorporation of Eu^{2+} into Ca-bearing minerals, and a smooth attenuation due to ionic size.

Volatility-controlled fractionations result from the different volatilities and speciation of the REE in nebular gas. A schematic illustration of these effects is shown in Figure 7. With the exception of Yb, present mainly as the monatomic vapor, and Ce, present mainly as CeO_2 gas with a minor fraction as CeO gas, the major REE gases in the solar nebula are the monoxides. Temperature-dependent partitioning of the REE between nebular gas and refractory minerals is controlled by condensation into solid solution in a host phase such as perovskite (or hibonite) via net thermochemical reactions exemplified by

$$LaO\ (g) + 0.5H_2O\ (g) = LaO_{1.5}\ (\text{in } CaTiO_3) + 0.5H_2\ (g)$$

for REE present dominantly as monoxide vapors,

$$Yb\ (g) + 1.5H_2O\ (g) = YbO_{1.5}\ (\text{in } CaTiO_3) + 1.5H_2\ (g)$$

for monatomic Yb, and

$$CeO_2\ (g) + 0.5H_2\ (g) = CeO_{1.5}\ (\text{in } CaTiO_3) + 0.5H_2O\ (g)$$

for most of Ce that is present as CeO_2 (g).

The Gibbs energies for the different condensation reactions do not vary smoothly across the lanthanide series. As a result, the partitioning of REE between gas and grains is irregular, with the LREE generally being more volatile than the HREE. Thermodynamic calculations predict that Eu, Ce, and Yb are the most volatile REE, and that Lu, Er, and Ho are the most refractory REE in nebular gas (e.g., Kornacki and Fegley, 1986). Because of the importance of CeO_2 gas, Ce partitioning between gas and grains is sensitive to the oxidation state of the surrounding environment, with more oxidizing conditions leading to less Ce being incorporated in condensed phases at a given temperature.

CAIs have played a major role in the search for isotopic vestiges of presolar material. Of paramount importance in the search for isotopic anomalies was the discovery of widespread anomalies in O isotopes (Clayton et al., 1973), likely caused by excess ^{16}O, at a level of up to 5% enrichment in Allende anhydrous materials. The characteristic feature on the oxygen three-isotope diagram is a slope 1 mixing line, as opposed to the slope 1/2 terrestrial mass fractionation line, between different mineral species from individual CAIs (Fig. 8A). Spinel and fassaitic pyroxene are the most enriched minerals, whereas melilite and anorthite are close to normal in composition. This behavior has been modeled as: (1) production of an ^{16}O-rich reservoir; (2) crystallization of CAIs in equilibrium with that reservoir; followed by (3) back-reaction in the solar nebula with re-equilibration dependent upon the individual minerals. A small subset of inclusions (FUN inclusions, see below) have an additional step in that they require the production of a mass-fractionated composition prior to back-reaction with isotopically normal O (Fig. 8B). Thus the third most abundant element in the solar system has an extremely large isotopic anomaly, requiring extreme heterogeneity in the solar nebula. The concept of a simple, completely vaporized, homogeneous cloud of solar gas is untenable. At the very least, a progressive change in the isotopic composition of the material being processed in the solar nebula is required.

Following the discovery of oxygen isotope effects, a major effort was instigated in solid-source mass spectrometry. Quantities of material required for analysis on thermal ionization mass spectrometers fell from micrograms to nanograms, and precision capability improved from percent to per mil and then to ε unit (10-4). These advances made possible isotopic analysis of Mg (Gray and Compston, 1974; Lee and Papanastassiou, 1974), which led to the discovery of the extinct radionuclide ^{26}Al in Allende

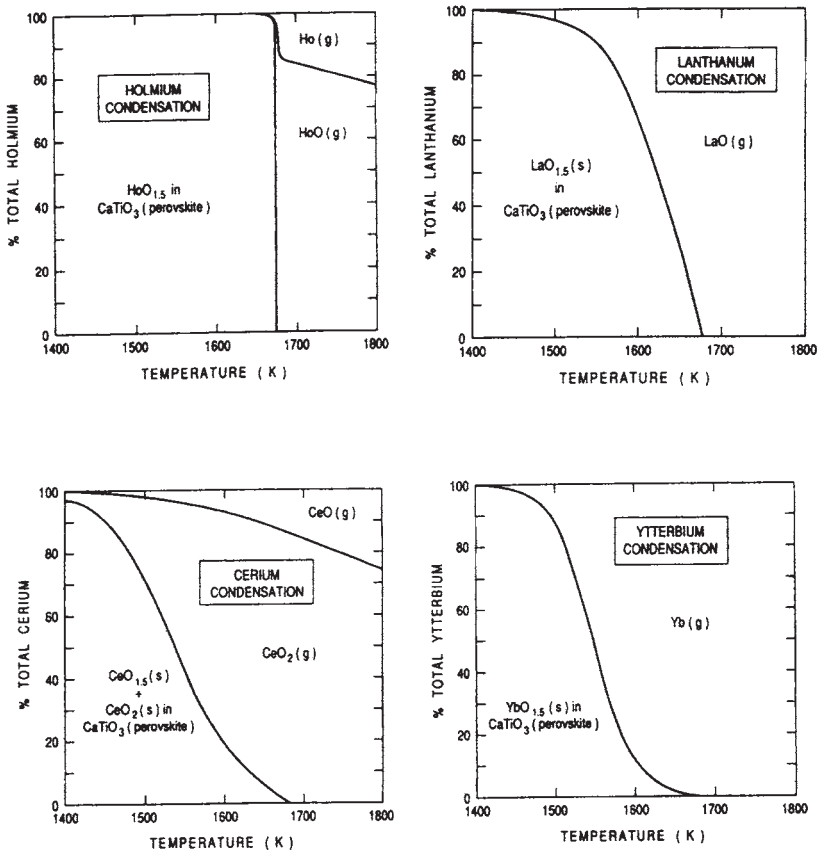

FIG. 7. Equilibrium chemistry of Ho, La, Ce, and Yb in the solar nebula at 10^{-3} bar total pressure. These four plots exemplify condensation of ultrarefractory (Ho), refractory (La), oxidizable (Ce), and volatile (Yb) REE. Methodology for the condensation calculations is described by Kornacki and Fegley (1986).

CAIs (Lee et al., 1977). Then excesses in ^{50}Ti were quantified (Heydegger et al., 1979; Niederer et al., 1980; Niemeyer and Lugmair, 1981) and thenceforth excesses in heavy isotopes of other elements of the Fe abundance peak, viz. Ca, Cr, Fe, Ni, and Zn (Birck and Allègre, 1984; Jungck et al., 1984; Birck and Lugmair, 1988; Loss and Lugmair, 1990; Völkening and Papanastassiou, 1989, 1990; Fig. 9).

The excesses in the n-rich isotopes of these elements have been interpreted as representing the addition of neutron-rich material from near the mass cut of a supernova into the solar system. The multiple-zone mixing model of Hartmann et al. (1985) is particularly successful in predicting the abundances of ^{48}Ca, ^{50}Ti, and ^{54}Cr in terms of material that has experienced large neutron excesses in a Type II supernova. However, Meyer et al. (1996) have indicated that the extreme entropy of the Type II supernova would likely bypass the lighter elements, and they postulate that most ^{48}Ca is produced in rare Type I supernova events.

In most Allende CAIs, the isotopic anomalies for the Fe abundance peak elements are typically of the order of 1‰. However, in a small subset of inclusions, larger isotopic anomalies are found. For example δ^{50}Ti in inclusion C1 is −4‰, whereas in EK1-4-1 it is +4‰ (Niederer et al. 1985), while EK1-4-1 has a ^{58}Fe excess of +29‰ (Völkening and Papanastassiou, 1989). These isotopic anomalies are associated with mass fractionation in the elements (i.e., the isotopes are also systematically fractionated according to their masses). The observation of similar effects in Mg, Si, and O led to these inclusions being termed FUN inclusions for their fractionated and

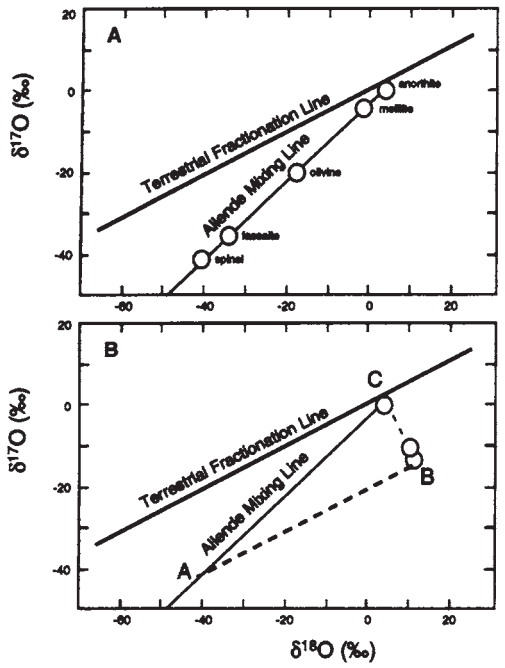

FIG. 8. A. Oxygen isotopic systematics for "normal" Allende CAIs. Minerals from an individual CAI, as well as bulk CAI measurements, define a mixing line with slope close to unity, in contrast to the slope 0.5 line defined by kinetic processing of oxygen isotopes on Earth (terrestrial fractionation line). These data suggest that CAIs formed from a reservoir enriched in ^{16}O by at least 50‰ relative to terrestrial abundances. Heterogeneity between minerals is probably related to reequilibration of melilite and anorthite with isotopically normal O, whereas spinel and fassaite (pyroxene) largely retain their initial composition (Clayton et al., 1977). B. Oxygen isotopic systematics for FUN Allende CAIs. These CAIs indicate an additional mass fractionation event that changes the initial composition from A to B followed by back-reaction with normal O at C. Data for the FUN inclusion HAL is shown (Lee et al., 1980).

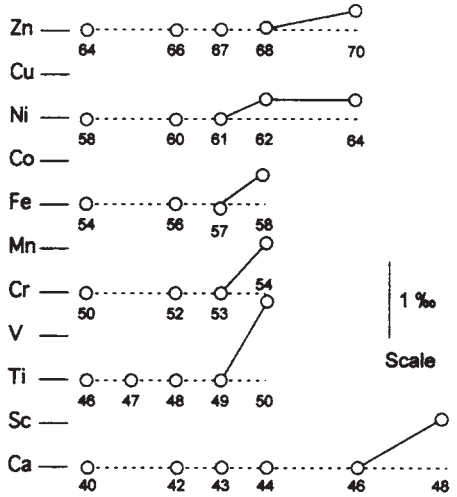

FIG. 9. Isotopic anomalies of the Fe group elements in "normal" Allende CAIs, showing enrichments of the heaviest isotopes of each element.

unknown nuclear components. For these elements, an unequivocal partitioning between the F and the UN effects may not be possible because the normalizing isotopes used for the mass fractionation determination could also be affected by the UN component. There are no distinguishing mineralogical characteristics for these inclusions to distinguish them from other "normal" Allende CAIs.

The isotopic compositions of other elements such as Sr, Zr, Ba, Nd, and Sm have also been measured from a limited number of Allende CAIs (see Lee, 1988). These elements too have a story to tell, but there are too few analyses for them to be used in a systematic way to address the formation of CAIs. Specific reference will be made to isotopic compositions of some of these elements in evaluating formation models.

Systematics of Allende CAIs

A common interpretation from Allende CAIs is that there is no systematic relationship between petrography, presence of $^{26}Al/^{27}Al$ at 5×10^{-5}, Ti isotopic composition, or ^{16}O enrichment (MacPherson et al., 1988). Nor are there any fundamentally distinctive characteristics of FUN inclusions. The FUN inclusions, with their large isotopic effects, are perhaps the most cited of any of the CAIs. Although these inclusions were extremely important in terms of initially documenting isotopic anomalies, their isotopic anomalies are now orders of magnitude less than those found in Murchison CAIs, at least in terms of the elements Ca and Ti. The coexistence of mass fractionation and nuclear anomalies in these inclusions is an interesting aspect, but so-called "normal" CAIs are still isotopically anomalous without the fractionation effects. Thus while the FUN inclusions are remarkable, their properties are not so unique as to require specific accommodations rather than just being within the continuum of CAI variations.

CAIs from the Murchison CM2 chondrite

Murchison is the most plentiful and accessible CM2 chondrite, so most analyses of CM2 CAIs are from this meteorite. There does not appear to be any marked distinction in the inclusions from Murchison compared to those from other CM2 meteorites. A feature of CM2 refractory inclusions is the widespread presence of hibonite ($CaAl_{12}O_{19}$), and rarely, the occurrence of corundum (Bar-Matthews et al., 1982; MacPherson et al., 1984, 1988; Hinton et al., 1988). Thus, these CAIs appear to contain assemblages that formed and were isolated from the nebular gas at an overall higher condensation temperature than Allende CAIs (e.g., see Fig. 1).

Murchison CAIs are typically of the order of 500 μm maximum dimension; thus they are difficult to analyze using the same methodologies as those originally employed in Allende CAI research. Sufficient material is available in an Allende CAI for neutron activation measurement of trace elements, and also for crushing, dissolution, and separation of the desired chemical species for mass-spectrometric isotopic analysis. The advent of ion microprobe analysis opened up Murchison CAIs to routine analysis for trace-element concentration as well as isotope measurements (see Ireland, 1995). The advantage of ion microprobe analysis is that analyses can be carried out *in situ*, allowing petrographic context to be utilized in selecting areas, even of a given mineral, for analysis. Thus for example, different generations of a single mineral can be analyzed. Ion microprobe analysis has sometimes been referred to as "virtually nondestructive," but this is demonstrably not the case for relatively small extraterrestrial objects such as these. The drawbacks of ion microprobe analysis are the requirements for high mass resolution to separate molecular isobars, and the relatively lower precision for ion microprobe analysis compared to some other mass spectrometric techniques. However, the panacea for ion microprobe analysis is that large isotopic variations can be found in CAIs, for which ultimate precision is not an issue.

A feature of Murchison CAIs is the common occurrence of blue hibonite. Hibonite is predicted to be the second major condensate phase after corundum from a cooling gas of solar composition. Perhaps the most distinctive type of Murchison CAIs are single grains of essentially pure hibonite that are transparent but display a blue pleochroism through thick sections. These have been referred to as DJ (blue chip) fragments (Hinton et al., 1988) or PLAC (PLAty Crystals; Ireland, 1988). However, the most common type of hibonite-bearing inclusions are those within spinel. These hibonites appear bright blue even as relatively small (typically 10 × 30 μm) inclusions. This type has been referred to as SHIB (Spinel-HIBonite; Ireland 1988). Other types of inclusion described include hibonite-glass inclusions, where the hibonite occurs as crystals within glass or devitrified glass of pyroxene composition (Ireland et al., 1991; Simon et al., 1998), and the HAL-type hibonite inclusions named after the Allende FUN inclusion (Ireland et al., 1992; Russell et al., 1998).

The chemistry of hibonite allows the substitution of Mg^{2+} and Ti^{4+} for $2Al^{3+}$ (Allen et al., 1978). In the PLAC hibonite, and in hibonite from glass inclusions, TiO_2 substitution typically reaches a maximum of 2 wt% TiO_2, but in SHIB hibonite, concentrations as high as 10 wt% are found (Ireland, 1990). The blue color of hibonite is related to the presence of a small amount of Ti^{3+} (direct substitution for Al^{3+}; Ihinger and Stolper, 1986). Thus the SHIB hibonites are the brightest blue because of the overall higher Ti concentration, and thereby higher Ti^{3+} concentration. The HAL-type inclusions are noteworthy in having relatively low Ti concentrations (< 1 wt % as TiO_2) and essentially no Mg.

The trace-element chemistry of Murchison CAIs like that in Allende is dominated by volatility-controlled fractionation, but is also distinctive in the petrographic hibonite groups. PLAC hibonites typically have a Group III-type pattern with depleted abundances of Eu and Yb relative to the other REE (Ireland et al., 1988; Fig. 10A). SHIB hibonites have patterns that are quite similar to the Group II pattern, with depleted abundances of the ultrarefractory REE compared to the light REE abundances (Fig. 10B), and a few have ultrarefractory-enriched compositions (Fig. 10C). In the Murchison inclusions, however, the more volatile REE Eu and Yb are more variable and, in some cases, even elevated beyond the light REE concentrations. The glass spherules have hibonite that is somewhat variable in composition, and the glass can have trace element abundances associated with equilibrium hibonite-melt distribution coefficients (Beckett and Stolper, 1994), but not always (Ireland et al., 1991). The HAL-type inclusions have strong depletions in Ce, which is a characteristic feature of distillation in an oxidizing environment (Ireland et al., 1992; Fig. 10D). Other inclusions can have relatively unfrac-

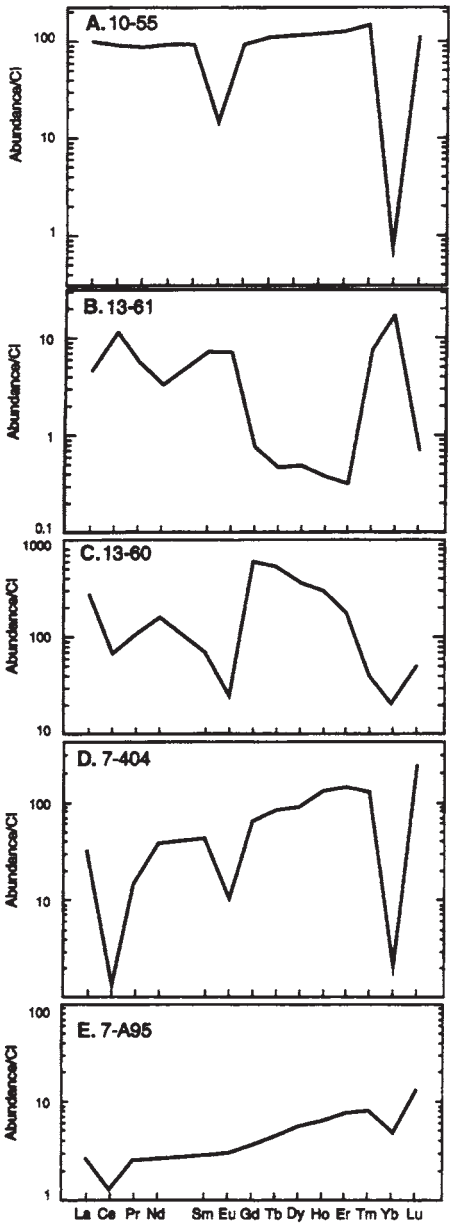

FIG. 10. REE abundance patterns from Murchison CAIs show anomalies in the abundances of the relatively volatile REE Ce, Eu, and Yb, as well as fractionations in the ultrarefractory REE ranging from depletions to enrichments.

tionated patterns with only minor anomalies in the more volatile REE (Fig. 10E).

Magnesium isotopic compositions most commonly show enrichments in ^{26}Mg due to ^{26}Al decay

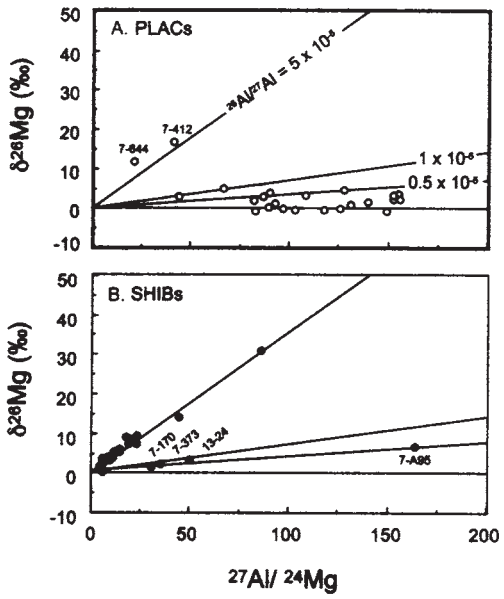

FIG. 11. Al-Mg isochron diagrams for Murchison CAIs. In general, PLAC hibonites show little or no excess ^{26}Mg due to the decay of ^{26}Al, whereas SHIBs show $^{26}Al/^{27}Al$ at the canonical solar system abundance of 5×10^{-5}.

with a bimodal distribution between the canonical solar system $^{26}Al/^{27}Al$ of 5×10^{-5} for SHIB inclusions to $< 1 \times 10^{-5}$ for PLAC inclusions (Fig. 11). The glass spherules are typically nonradiogenic (i.e., low apparent initial $^{26}Al/^{27}Al$), and some inclusions have initial $^{26}Mg/^{24}Mg$ ratios that are lower than the terrestrial ratio (Ireland et al., 1991). The HAL-type inclusions have very low Mg concentrations and therefore have high Al/Mg ratios, which facilitates measurements of initial $^{26}Al/^{27}Al$. The HAL-type inclusions show variable inferred $^{26}Al/^{27}Al$, and also mass-fractionated Mg isotopes consistent with evaporation of Mg (Ireland et al., 1992).

Calcium and titanium isotopic compositions are the most anomalous in PLAC inclusions (Ireland, 1990), whereas most SHIB inclusions are within error of normal. The pattern is similar to that for Allende CAIs—that is, the anomalies are in the heaviest, most neutron rich isotopes. However, the size and range of the anomalies are much larger. Enrichments in ^{50}Ti and ^{48}Ca range up to 270‰ and 100‰, respectively, while depletions also are common, with the largest being −70‰ and −60‰ for ^{50}Ti and ^{48}Ca, respectively (Zinner et al., 1986; Hinton et al., 1987; Ireland, 1990). Anomalies in ^{49}Ti

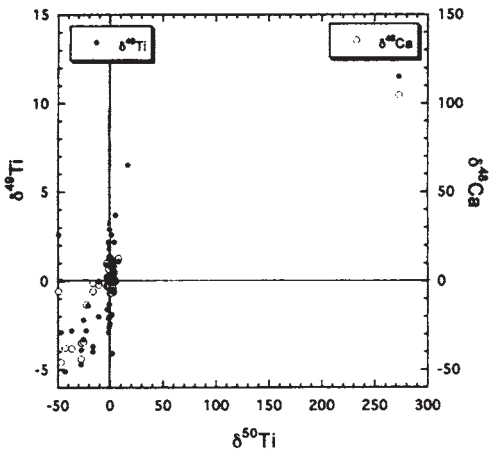

FIG. 12. Ca-Ti isotopic compositions in Murchison hibonites show extreme compositions compared to the Allende inclusions. Data for δ^{49}Ti and δ^{48}Ca are plotted against δ^{50}Ti. Both ^{49}Ti and ^{48}Ca anomalies are well correlated against ^{50}Ti. Selected data from Ireland (1990) and Zinner et al. (1986).

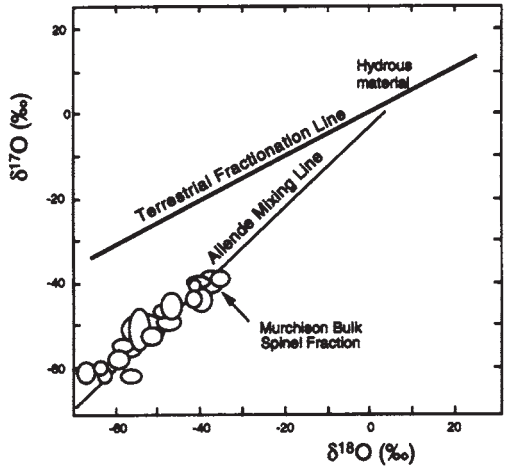

FIG. 13. O isotopic compositions in hibonite-bearing inclusions from Murchison show larger ^{16}O excesses than Allende CAIs extending down the Allende mixing line to ~70‰ excess levels.

are smaller but are well correlated with ^{50}Ti anomalies (Fig. 12). The glass inclusions have moderately variable Ca and Ti isotopic compositions, whereas the HAL-type inclusions typically have mass-fractionated Ca and Ti isotopes but relatively small "non-linear" effects after removal of the mass fractionation component.

Oxygen isotopic compositions (Fahey et al., 1987; Ireland et al., 1992) are not distinctive between the various groups and all show the large apparent ^{16}O effect seen in Allende CAIs (Fig. 13), albeit at a higher level of ^{16}O excesses, maximizing at around 70‰ as opposed to Allende CAIs at 50‰. Murchison CAIs are also affected by mixing, with a more normal isotopic component yielding variable compositions close to the Allende mixing line. HAL-type inclusions show isotopic fractionation away from the Allende mixing line, followed by mixing with isotopically normal material (i.e., the characteristic FUN inclusion systematics).

Systematics of Murchison CAIs

Murchison CAIs show a very strong polarization of morphological, chemical, and isotopic features between PLACs and SHIBs. PLACs have Group III–dominated REE patterns, while SHIBs are commonly Group II or ultrarefractory enriched. PLACs are the dominant source of Ca and Ti isotopic anomalies; only one SHIB is highly anomalous. Hutcheon et al. (1983) first noted the exclusivity of ^{26}Al and Ti isotopic anomalies in hibonite inclusions. This is largely a manifestation of PLAC hibonites, which have most of the large Ti isotopic anomalies, and do not contain excess ^{26}Mg. There is a propensity for inclusions with Group II–type patterns to have $(^{26}Al/^{27}Al)_0$ of 5×10^{-5}, but this does not hold as strongly as the likelihood of SHIB inclusions to have Group II REE patterns and ^{26}Al/^{27}Al at 5×10^{-5}, and PLAC hibonites to lack ^{26}Al. This is particularly noted for SHIB 7-170, which has a Group II pattern, but also has a large ^{50}Ti deficit and therefore no apparent ^{26}Al.

The correlation of ^{26}Al with Group II REE patterns is largely a manifestation of SHIB inclusions. However, this is not entirely the case, and there are several PLACs with Group II patterns and excess ^{26}Mg at $5 \times 10^{-5} \times {}^{27}$Al. Similarly, some SHIB hibonites possess rather flat REE patterns and do not have canonical radiogenic Mg.

Even within the types of hibonite, two morphologically very similar inclusions can exhibit quite different isotopic systematics. For example, 7-734 and 7-170 (from Ireland, 1990) are morphologically the same, with hibonite-spinel cores surrounded by a rim sequence. However, 7-734 is a typical SHIB with Group II REE pattern, ^{26}Al/^{27}Al of 5×10^{-5}, and normal Ti isotopic composition. In contrast, 7-170 is the most unusual SHIB with a Group II REE pattern but no radiogenic ^{26}Mg excess, and a ^{50}Ti deficit of ~50‰. Thus the morphological and petro-

graphic distinctions of PLACs and SHIBs largely reflect variations (pressure, temperature, gas composition) between volumes of the solar nebula in which the inclusions formed. SHIB 7-170 probably has included a proto-CAI that has more similarities to PLACs than to the typical Ti isotopes and Al-Mg systematics of SHIBs. But with thermal processing in the SHIB region, the PLAC-type precursor has been absorbed into the new CAI. The question then becomes, which of the components really are linked. Is the SHIB region dominated by Group II REE and $^{26}Al/^{27}Al$ of 5×10^{-5} and normal Ti with only a few seed inclusions that bring in inherited components such as the Ti and Al-Mg in 7-170? An interesting test would be to measure the Mg associated with 7-170 spinel to see if its composition is consistent with other SHIB Al-Mg at $^{26}Al/^{27}Al$ of 5×10^{-5}.

Even though there is some consistency between the groups of hibonites, there is a wide range of chemistry and isotope compositions that needs to be evaluated against one another. Although isotope systematics can be represented as a numerical value of an isotopic anomaly, REE have more generally been referred to in terms of the canonical REE groups. But the assignment to a group is rather subjective, and some inclusions bear attributes that are not found in any of the Allende REE patterns. As such we have developed a numerical scheme for quantifying REE characteristics of CAIs.

As previously noted, REE patterns in CAIs are the result of at least three different fractionation events. The volatility-controlled fractionations affecting the most refractory and the most volatile elements of the refractory lithophile sequence are of most use for classification purposes, whereas of minimal use is the magmatic fractionation between different phases. Fractionation in the most refractory elements is responsible for Group II patterns and the attribute that is commonly used to describe the Group II pattern is the presence of a Tm anomaly. This can be numerically defined as Tm/Tm*, where Tm* refers to the interpolated value between the Er and Lu CI-normalized abundances.

The more volatile lithophile elements could be represented by either Eu or Yb. We prefer to use Yb because of the possible fractionation of Eu^{2+} between Ca-bearing phases. However, calculation of Yb/Yb* is not straightforward because of the possible superposition of the ultrarefractory fractionation. In terms of the volatile-element fractionation, a more useful reference point is the light REE. But to use the LREE, a substantial extrapolation is required, and it might also be compromised by variability in the LREE abundances such as in Murchison ultrarefractory-fractionated CAIs. However, as found in Allende Group II patterns, Tm is a good proxy for the LREE. Thus we use the CI-normalized Yb/Tm ratio to express the volatile-REE fractionation.

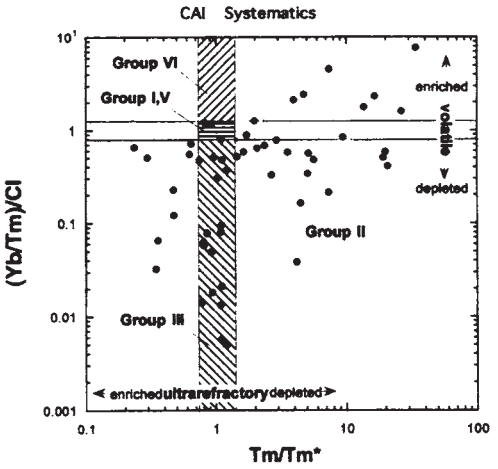

FIG. 14. REE classification of CAIs based on Tm and Yb anomalies to quantify ultrarefractory REE fractionation and volatile REE fractionation, respectively. Yb is used rather than Eu because of the propensity of Eu to exist in the Eu^{2+} oxidation state and be partitioned during magmatic processes into Ca-bearing phases. Tm is used as the reference element because it behaves as a LREE and provides a better estimate of volatile fractionation in the HREE. Tm* is calculated from the interpolated value between Er and Lu. Yb/Tm is normalized to the CI value such that (Yb/Tm) CI is the solar value. Shown on the plot are the regions where the Allende CAI patterns (Fig. 4) occur.

Data from approximately 50 Murchison CAIs, from Ireland et al. (1988) and Ireland (1990), are presented in this classification scheme in Figure 14. Allende CAIs of Groups I, III, V, and VI have no Tm anomalies and show variation only in Eu and Yb abundances. The positions these groups plot are shown in the hachured regions. Group II inclusions from Allende show depletions in both ultrarefractory and volatile REE, and hence plot in the lower right region of the diagram. Murchison CAIs cover a large range of this diagram, ranging from ultrarefractory enriched to depleted and volatile enriched and depleted. However, most inclusions are volatile-REE depleted and the only inclusions strongly enriched in these elements also show the strongest

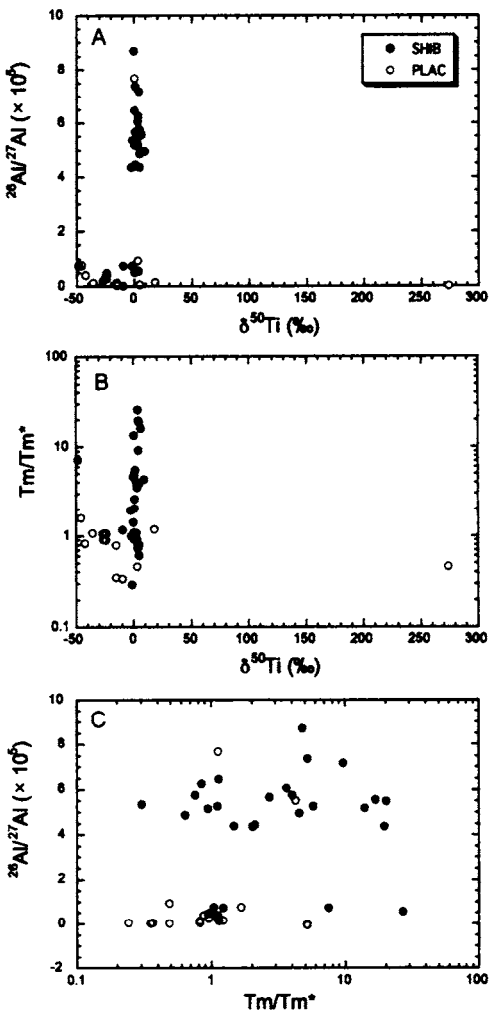

FIG. 15. Chemical and isotopic systematics of Murchison CAIs. Spinel-hibonite (SHIB) and single crystal fragments (PLAC) inclusions are quite polarized in their systematics. A. Ti anomaly versus inferred ^{26}Al abundance. Most Ti isotopic anomalies are found in PLACs but no inclusion has both large (> 10‰) ^{50}Ti anomaly and $^{26}Al/^{27}Al$ of 5×10^{-5}. B. Ti anomaly versus Tm abundance. PLAC and SHIB hibonites largely plot on orthogonal trends because of the propensity for SHIB to show ultrarefractory fractionations but no Ti anomalies, whereas PLAC have variable Ti isotopic compositions and more commonly volatile REE fractionation (Group III). C. ^{26}Al abundance vs. Tm anomaly. The bimodality of inferred initial ^{26}Al is apparent, but there is no distinct correlation between REE fractionation and ^{26}Al abundance despite SHIB hibonites dominating the ^{26}Al-rich inclusions. Ultrarefractory-element fractionations are also present in PLAC with low ^{26}Al abundances.

Tm anomalies. No inclusion with an ultrarefractory enriched pattern also has enriched volatile elements.

With a numerical quantification of REE patterns, isotopic compositions can be compared to the trace element systematics. The exclusivity of Ti isotopic anomalies and inferred ^{26}Al is shown in Figure 15A. In Figure 15B, Ti isotopic anomalies are plotted against Tm anomalies. The ultrarefractory-fractionated SHIB patterns produce a vertical pattern around the normal Ti isotopic composition, whereas the PLACs with diverse Ti isotopic compositions have more normal Tm abundances. In Figure 15C, bimodality of inferred ^{26}Al abundance is clearly apparent, but no correlation exists between Tm abundance and inferred ^{26}Al at a level of $5 \times 10^{-5} \times {}^{27}Al$.

The Early Solar System

High-temperature processes

The formation of CAIs in a hot, cooling solar nebula is consistent with the models for solar nebula formation proposed by Cameron (1962). Basically, gravitational in-fall produced sufficient kinetic energy to vaporize all solid materials. The widespread absence of isotopic anomalies in solar system materials, as measured at that time, was entirely consistent with such a view (Suess, 1965). Up until the discovery of ubiquitous isotopic anomalies in oxygen, isotopic variations had only been described from volatile elements such as H, Ne, and Xe (Reynolds, 1967) and those anomalies could be ascribed to late-stage in-fall of some exotic material that had escaped homogenization. However, the high-precision measurement of O isotopic compositions in Allende CAIs substantially changed this concept. At the very least, two major isotopic reservoirs were required to accommodate O isotopic compositions. Further isotopic variability in elements such as titanium require preservation of the isotopic integrity of much smaller amounts of material. While high temperatures are required to form the condensation-fractionated REE patterns, not all material could have been vaporized because isotopic heterogeneity would have been quickly removed.

Preservation of isotopic anomalies

In essence, the concept of an isotopic anomaly is rather misleading. The isotopic abundances of the elements in the solar system are sourced from many different nucleosynthetic sites, and those sites have

specific physical and chemical conditions that drive nuclear reactions in specific ways. Thus our reference frame for examining isotopic compositions is the average of all the material from all sites that has come into the source region for Earth. As such, there is nothing especially significant about the exact mix that is present on Earth. There is even a distinct likelihood that radial variations exist in the solar nebula for certain isotope abundances, particularly those for elements that exist in volatile components. Determining isotopic anomalies is an attempt at unmixing some of the isotopic components that have not been completely homogenized during the mixing phases of the solar nebula. We use the average terrestrial isotopic compositions of the elements simply as a useful reference point to begin.

The concept of isotopic anomalies has changed over the years from the attempts to measure isotope abundances that differ from the terrestrial abundances by only small amounts, to one of characterizing distinct nucleosynthetic compositions in grains that have likely crystallized around another star. In this case, there is nothing particularly anomalous in the composition of the grain in its local neighborhood of formation, although its composition may differ greatly from that of terrestrial isotopic compositions. The isotopic composition of the grain simply reflects the mix of components that have contributed to the star, possibly augmented by nucleosynthesis in the star. As such, referencing the isotopic composition to terrestrial abundances may give a misleading inference as to the anomalous isotope component(s) present. Where anomalies are large, a specific comparison with terrestrial abundances can be dropped, and the ratios alone can be sufficiently diagnostic to allow association with a specific source. When the isotopic deviations are smaller, it may be more difficult to assign a specific component that characterizes the anomalous material.

Further complicating the assignment of anomalous components is the presence of deficits of certain isotopes relative to the terrestrial composition. A case in point is the presence of apparent deficits in ^{50}Ti in hibonite, which is complementary to large ^{50}Ti excesses. The interpretation of ^{50}Ti as the anomalous isotope is beyond question. The abundances of the light isotopes of Ti are typically within the range of normal terrestrial Ti, but more importantly, there is no difference in these abundances for compositions with large ^{50}Ti excesses compared to those with ^{50}Ti deficits. But, while a ^{50}Ti excess can simply be expressed as a number of atoms of ^{50}Ti in excess of that observed for isotopically normal Ti, the deficit cannot be represented as a negative number of atoms because such a number has no physical basis.

The interpretation of such isotopic deficits places greater constraints on the interpretation of isotopic anomalies than the interpretation of excesses. In the case of ^{50}Ti again, Hinton et al. (1987) proposed that the inclusion with the greatest deficit, BB-5 at $-70‰$, actually represented the original Ti-isotopic base composition for the solar nebula, and the present terrestrial ratio was augmented by the addition of a spike of isotopically anomalous Ti as represented in the inclusions with large enrichments in ^{50}Ti. This concept is part of the Late Supernova Injection (SNI) model originally proposed to account for excesses in ^{16}O and ^{26}Al in the early solar system, as produced by a supernova in close proximity to the solar nebula (Cameron and Truran, 1977). Thus, isotopic components were added to the solar system, which was originally depleted in these isotopes relative to the present. The base composition for any element is represented by the most depleted composition for the given isotope of that element. However, Fahey et al. (1987) dismissed the case for the SNI model for the deficit in ^{50}Ti because BB-5 has an ^{16}O excess that is even larger than the most ^{50}Ti-enriched hibonites. The base composition for ^{50}Ti is associated with an enriched ^{16}O composition, not the base composition of oxygen which would be expected for the SNI model. This behavior indicates uncorrelated behavior of O and Ti isotope systems.

An alternative interpretation of the Ti isotope depletions is that the inclusions contain isotopic components inherited from the site of nucleosynthesis, and have been preserved through the high-temperature processing in the solar system. This chemical memory model (Clayton, 1982) is relevant to all isotopic variations, and simply states that material can survive the extreme mixing and homogenization processes in the early solar system. In this case, refractory elements such as Ca, Ti, and Mg are more likely to preserve isotopic effects because they are less likely to be processed into the gas phase where isotopic variations may be easily homogenized.

Oxygen-16

Enrichments in ^{16}O in CAIs are a ubiquitous feature. In fact, the ubiquity of ^{16}O enrichments at basi-

cally the same level in all CAIs is rather puzzling. Despite wide variability in other isotopic systems such as Ti, oxygen is rather uniform. This is despite highly anomalous oxygen isotope systematics of putative presolar grains (Nittler et al., 1997; Choi et al., 1999), indicating that exotic O isotopes were present in the solar system mix originally.

Clayton et al. (1973) found that the extreme enrichment in Allende material was approximately 50‰ (relative to the intersection of the Allende mixing line and the terrestrial mass fractionation line which is at +10‰). Clayton and Mayeda (1984) found similar enrichments in Murchison refractory separates, although more extreme compositions with enrichments up to 70‰ have been found in some Murchison inclusions (Fahey et al., 1987; Virag et al., 1991; Ireland et al., 1992). The extreme compositions show evidence for back-mixing with a more normal oxygen isotopic composition, and the composition of a mineral is apparently related to its susceptibility to resist O equilibration by diffusion (Blander and Fuchs, 1975; Ryerson and McKeegan, 1994). Melilite and anorthite typically have more normal oxygen isotopic compositions than pyroxene, while spinel and hibonite typically show extreme enrichments. However, the nature of these isotope effects is not easily explained in terms of diffusion because diffusion gradients that should be observed are not there (Ryerson and McKeegan, 1994; McKeegan et al., 1998). FUN inclusions also show ^{16}O enrichments, but they are complicated by an apparent mass-dependent fractionation from the ^{16}O-enriched reservoir along a line of slope 1/2 (i.e., mass-dependent fractionation), followed by back-reaction with a near-normal component.

Excluding FUN CAIs, variable replacement of oxygen thus results in the CAI mixing line being located between the exotic ^{16}O-enriched component and the normal compositions. Best-fit slopes of these lines typically have been approximately 0.95, although microanalysis of CAIs suggests a slope of 1.00 (Young and Russell, 1998). The distinction between slope 0.95 and 1.00 is important for the two main competing mechanisms for production of an ^{16}O-enriched reservoir. The original interpretation of the ^{16}O-rich reservoir is that it represents a nucleosynthetic enrichment in the early solar system, possibly related to the supernova responsible for ^{26}Al production (Clayton et al., 1973, 1977).

An alternative explanation proffered by Thiemens and Heidenreich (1983) is that oxygen isotopes can undergo mass-independent fractionation because of differing molecular stability of nonsymmetric (e.g., $^{16}O - C - ^{17}O$) versus symmetric (e.g. $^{16}O - C - ^{16}O$) molecules (e.g., Thiemens, 1996). This or another mechanism occurs in the Earth's atmosphere, where mass-independent O isotope fractionations are observed in O_3, CO_2, and other O-bearing molecules. Chemical fractionation is thus a highly attractive model for explanation of the ^{16}O enrichment. However, an explicit illustration of the applicability of non–mass-dependent fractionation in the solar nebula has not been demonstrated. In particular, CAIs form at high temperature, where these mechanisms may not be viable, and gas-solid fractionations are important as opposed to gas-gas fractionation. Nevertheless, the viability of this mechanism is implicit upon a fractionation slope of exactly 1.00. If the slope of 0.95 were real, the exotic composition would be required to have an anomalous $^{17}O/^{16}O$ (or $^{18}O/^{16}O$) to explain the exotic reservoir, which cannot be explained by the mass-independent fractionation model. However, the presence of a slope 1.00 mixing line does not preclude the presence of a pure ^{16}O-rich nucleosynthetic reservoir.

Aluminium-26

The nature of ^{26}Al abundances in solar system materials has been reviewed recently by MacPherson et al. (1995). The main feature of the Al-Mg systematics of refractory inclusions is the rather well defined upper cutoff of 5×10^{-5} for $(^{26}Al/^{27}Al)_0$. This upper limit is very important and has several fundamental implications for the incorporation of ^{26}Al into the solar system.

The source of the ^{26}Al is still a matter of conjecture. Supernovae produce ^{26}Al at a level of $10^{-3} \times {}^{27}Al$ (Clayton and Leising, 1987) and a supernova source would suggest that there is a decay interval of approximately 3 Ma while the $^{26}Al/^{27}Al$ ratio decayed from 10^{-3} to 5×10^{-5}. However, the gamma line for ^{26}Al decay has been detected coming from the galactic center at an abundance that cannot be produced entirely by supernovae. Presolar SiC grains contain inferred ^{26}Al at levels higher than produced in supernovae, with mainstream SiC having ratios up to 10^{-3} or so, and grains that may have a supernova origin having ratios up to 0.2 (Amari et al., 1992). The rare presolar oxide grains, corundum and hibonite, also show large excesses in Mg, corresponding to a similar range as found in carbide grains (Virag et al., 1991; Choi et al., 1999). The presolar grains certainly indicate that there are suit-

able nucleosynthetic sources. However, in order to achieve a uniform abundance, the source would have to have a fixed production ratio and there would have to be a fixed decay interval for travel from the point of nucleosynthesis to the solar system and then crystallization in solid objects. A scenario incorporating a variable production ratio compensated by different decay intervals is too abstruse to be a viable mechanism. The maximum production ratio indicated from the presolar grains (0.2) indicates a maximum decay interval of 12 half-lives, or approximately 9 Ma, to achieve a solar system $^{26}Al/^{27}Al$ of 5×10^{-5}.

Additional temporal constraints come from ^{41}Ca. The half-life of ^{41}Ca is only 0.1 m.y., and its abundance in the early solar system is estimated to be $1.5 \times 10^{-8} \times {}^{40}Ca$ (Srinivasan et al., 1994, 1996). The production ratio of ^{41}Ca has been estimated at $0.01 \times {}^{40}Ca$ (Wasserburg et al., 1995), and a value very similar to this has been measured directly from presolar graphite grains (Amari et al., 1992). This production ratio suggests a decay interval of the order of 19 half-lives, or 1.9 m.y., to achieve the 1.5×10^{-8} solar system value. Wasserburg et al. (1995) evaluated a common source for ^{41}Ca and ^{26}Al from an AGB star and used additional constraints from other radionuclides such as ^{60}Fe and ^{107}Pd. They conclude that the decay interval can only be of the order of 0.5 m.y. for internal consistency of these chronometers in CAIs. At this time, the source would have had a $^{26}Al/^{27}Al$ of 8×10^{-5} and a $^{41}Ca/^{40}Ca$ of 5×10^{-7}, based on the apparent measured values in CAIs.

The possibility of producing ^{26}Al *in situ* in the early solar system through T-Tauri radiation or the like has been examined, but does not produce the different radionuclides (^{26}Al, ^{41}Ca, ^{53}Mn, ^{60}Fe, etc.) in the predicted abundances (Wasserburg, 1985; Wasserburg et al., 1995; Shu et al., 1996; Lee et al., 1998). This may reflect uncertainties in the modeling of the radiation processes or that different nuclides have different relative contributions from *in situ* production and fresh nucleosynthetic injection. A case in point is the recent discovery of $^{11}B/^{10}B$ anomalies, which indicate the presence of ^{10}Be in CAIs (McKeegan et al., 2000) that can only have a spallogenic source, because ^{10}Be is consumed in stars, not produced. Nevertheless, the presence of spallogenic Be still does not preclude the presence of nucleosynthetic contributions in other elements. Another difficulty for modeling *in situ* production of an isotope is that the target nuclei are generally other elements, and so different chemical compositions can result in different apparent initial ratios.

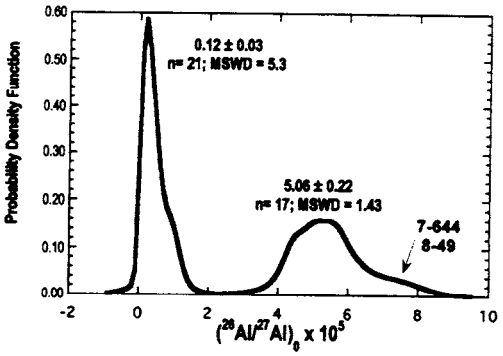

FIG. 16. Probability density function for ^{26}Al abundance in Murchison CAIs. Data are included only for CAIs with $^{27}Al/^{24}Mg > 10$. Two inclusions have marginally high $^{26}Al/^{27}Al$ values with respect to the main peak at $\sim 5 \times 10^{-5}$, but 17 inclusions are consistent with a single value at 5.06 ± 0.22 ($2\sigma_m$). Inclusions with low apparent initial ^{26}Al show a larger degree of scatter.

Even with a uniform production ratio of the radiogenic nuclide, a uniform distribution in the proto-CAIs is not guaranteed, nor even expected. The preservation of isotopic anomalies suggests that packets of dust were processed in the solar nebula at high temperatures to produce melting and thence crystallization. Any old Al (i.e., pure ^{27}Al) present in that package will produce a lower apparent initial $^{26}Al/^{27}Al$. Thus the expectation for the distribution of ^{26}Al is that the maximum will only be attained when the CAI consists predominantly of freshly injected material. Thus the distributions shown by MacPherson et al. (1995) are unusual, in that there is a clear peak at 5×10^{-5} and another peak closer to zero, with some intermediate values. However, it is not clear whether these intermediate values are the result of disturbance, stochastic variability associated with low Al/Mg ratios, or temporal decay. Of great importance in assessing this behavior will be the abundance of ^{41}Ca in these inclusions because the shorter half life of ^{41}Ca will effect an exponential change in the abundance, whereas dilution or disturbance of ^{26}Al will produce a linear change of the same magnitude in ^{41}Ca. The main problem is that the abundance of ^{41}Ca is already difficult to measure at the 10^{-8} level, and the relative quantification between the predicted exponential decay and the linear dilution may be beyond present analytical capabilities.

Thus the maximum $^{26}Al/^{27}Al$ is the salient point of CAIs because any old ^{27}Al can simply dilute the solar $^{26}Al/^{27}Al$ to a lower value. CAIs can also be disturbed in terms of their Al-Mg systematics through redistribution of Mg in subsequent thermal processing. It is in fact surprising that so many CAIs do preserve a common $^{26}Al/^{27}Al$. This property is exemplified in Figure 16, which shows the probability density function for $^{26}Al/^{27}Al$ values of 40 Murchison hibonites analyzed by Ireland (1988, 1990). The pattern is essentially bimodal, consisting of CAIs with low $^{26}Al/^{27}Al$ ($< 10^{-5}$) and those around 5×10^{-5}. The populations are somewhat biased because the probability density function is binned in intervals of 1×10^{-6}, and hence the low values are contained in a fewer number of bins, which increases the height of the function.

Furthermore, the low $^{26}Al/^{27}Al$ values come from hibonites with high Al/Mg and are often free of spinel (PLACs), thus producing narrow gaussian profiles. SHIBs which contribute most of the 5×10^{-5} peak are characterized by having small hibonite crystals with lower Al/Mg, sitting in a spinel matrix and thus the measurement errors for SHIBs can be relatively high in terms of $^{26}Al/^{27}Al$. The peak with elevated $^{26}Al/^{27}Al$ has a mean of $5.06 (\pm 0.22\ 2\sigma_m) \times 10^{-5}$ with an MSWD of 1.43. Two inclusions, 7-644 and 8-49 with apparently higher $^{26}Al/^{27}Al$, have been removed from the calculation. Nevertheless, the low MSWD for the remainder indicates that the analytical errors are largely consistent with there being only one component present. Even the standard deviation about this peak is only 1×10^{-5}.

Thus, CAI formation must occur over a very short interval of time, much less than one half-life of ^{26}Al (= 0.7 m.y.). It appears that the CAI data set we have comes from a temporally distinct period in the solar system. CAIs with low $^{26}Al/^{27}Al$ probably do not have temporal significance because of the possibility of adding old ^{27}Al associated with residues (as noted above). What is surprising is that there is no indication of more continuous mixing between these populations.

Trace-element fractionations

As noted above, the mineralogy of CAIs is consistent with high-temperature formation. But the chemical and isotopic systematics tell us more. The Group II pattern in particular is construed to be a condensate pattern and requires the separation of the most refractory elements in the first condensates and their removal from the locale prior to condensation of the Group II REE, which in turn must be isolated prior to condensation of the most volatile REE, Eu, and Yb (Boynton, 1975). The complementary ultrarefractory enriched pattern is found in some Murchison inclusions as well as in CAIs from other meteorites, although notably not Allende. The ultrarefractory pattern could be an early condensate removed from the gas phase, or a residue of material that was not quite completely evaporated. Isotopic-mass-fractionation measurements of hibonite-bearing inclusions show that on average, those with ultrarefractory-enriched patterns tend to have isotopically heavier Ti isotopes than those with the Group II (ultrarefractory-depleted patterns) (Ireland, 1990). This alone does not exclusively distinguish between a residue and condensate origin for the ultrarefractory-enriched material. The relative degrees of isotopic fractionation for either condensate or residue are a function of the composition of the starting material. Thus a residue will always be isotopically heavier than the starting material and will get heavier as evaporation continues. But the condensate evaporating from a residue will also become progressively heavier as the residue becomes heavier. Thus a late-stage condensate can ultimately become heavier than the original material.

The volatility fractionation of the REE and the other refractory lithophile elements has never been demonstrated experimentally and the ordering of these elements is largely based on a theoretically calculated volatility sequence modified using REE abundances from approximately 100 Allende CAIs (Kornacki and Fegley, 1986). That is, the ordering can be changed slightly so as to achieve the smoothest pattern of abundance versus condensation temperature. In detail, the apparent ordering can be compromised if significant fractionation of elements between two different phases takes place. This partitioning is a function of ionic radius; hence elemental abundances can change accordingly, and the resultant volatility sequence could change depending on the type of analysis that is carried out (for example, bulk analysis via INAA, or selected mineral analysis by ion microprobe). Trace-element partitioning appears as a smooth variation on the REE abundance pattern—for example, as a depletion of the REE with increasing ionic size in both hibonite and perovskite. This type of behavior is noticeable in hibonites with Group III patterns where the trend of the heavy REE is easily seen. The corresponding phase containing the heavy REE is typically not

TABLE 1. REE Classification of 396 CAIs

Meteorite	I, V	II	III	IV	VI	Ultra	UC	HAL	Total
Acfer 182[1,2]		17	1			3			21
Acfer 059 - El Djouf 001[1,2]		4							4
Allende[3]	54	36	12	3	6			1	112
Arch	1								1
Cold Bok.			2						2
Dhajala								1	1
Efremovka[4]	5	1					1		7
Essebi						1			1
Felix			1						1
Grosnaja	2								2
Kaba		1	7	12			2		22
Lancé	1	1							2
Leoville[4,5]	8	4			1				13
Mighei[6]	10	23	6				28		67
Mokoia		5							5
Murchison[7]	5	33	35			7		2	82
Murray	1	5	2			1			9
Ornans		1				3			4
Semarkona		1							1
Vigarano[4,5]	12	5	2				1		20
ALH85085[8]	2	12	2		1		2		19
Total	101	149	70	15	8	15	34	4	396
Percent	25.5	37.6	17.7	3.8	2.0	3.8	8.6	1.0	

[1]Weber et al., 1995.
[2]Weber and Bischoff, 1994.
[3]Simon et al., 1998.
[4]Sylvester et al., 1993.
[5]Sylvester et al., 1992.
[6]MacPherson and Davis, 1994.
[7]Simon et al., 1996.
[8]Kimura et al., 1993.

present with the PLACs, but the glass in hibonite-glass spherules can show the complementary HREE-enriched pattern (Ireland et al., 1991).

Such fractionation is more difficult to identify in ultrarefractory-depleted patterns because this pattern is already depleted in the HREE. It can, however, be very noticeable on the ultrarefractory-enriched pattern where there is commonly a distinct roll-off in the abundances of the heaviest REE, which are the most refractory and should have the highest normalized concentrations. Four inclusions analyzed by Ireland (1990) all have roll-offs in the abundances of the HREE, indicating the role of REE partitioning during melting. There is no phase containing the remaining REE in these inclusions, although occasional metal-rich nuggets and other "hot spots" can contain high concentrations of ultrarefractory REE (Palme et al., 1982; Hinton et al., 1988) and a small proportion of these objects can dramatically affect the REE systematics. CAIs with their full complement of ultrarefractory REE are relatively uncommon (e.g., MH-115, Boynton et al., 1980; ALH85085 CAI-143, Kimura et al., 1993); both show flat patterns in the HREE, which are elevated above LREE abundances.

The production of the Group II pattern requires removal of an ultrarefractory-REE host phase (e.g.,

perovskite) from the nebular gas within a few degrees of its condensation temperature (Davis and Grossman, 1979), and so any fractionation scheme based on volatility requires some mechanism for holding the gas at exactly the right temperature to produce the fractionation. In a sense, the fractionation of these elements is all but miraculous by this mechanism, but the Group II pattern is extremely common in CAIs. Fegley and Ireland (1991) compiled REE data from 280 CAIs from 19 chondrites and found that the Group II pattern was present in one-third of all CAIs (Table 1). Moreover, the Group II pattern is evident even in bulk Allende (Fegley and Kornacki, 1984), reflecting both the high abundance of refractory inclusions in this meteorite and the high proportion of Group II CAIs. This is despite the possible selection bias of larger Allende CAIs having Group I or V patterns. In Murchison, for which a more random selection of CAIs is taken, Group II and III patterns are subequal, and only a few Group I, V patterns are evident.

Despite the common occurrence of Group II patterns in Allende, the complementary ultrarefractory-enriched pattern has never been found in that meteorite. Almost all patterns showing ultrarefractory-enriched patterns come from hibonite- and perovskite-dominated CAIs rather than the silicate-bearing Allende CAIs, although ultrarefractory-enriched patterns are found in the Ornans CO3 chondrite. In Murchison CAIs, the Group II–type patterns show distinct differences from Allende Group II in that they contain substantially higher Eu and Yb, and also typically show variability in the light REE abundances.

The complementarity of the ultrarefractory-depleted and ultrarefractory-enriched patterns from Murchison CAIs can be seen through the addition of the normalized abundances of two CAIs, 13-60 and 13-61 (Fig. 17). The simple addition of these two inclusions shows no major anomalies and results in a smoothly fractionated pattern. Particularly noteworthy is the removal of variability in the LREE, which is also seen to be related to volatility. As such, the differential partitioning between the Group II (condensate) and ultrarefractory-enriched pattern allows an estimation of the relative volatility of each element. However, the addition of the logarithms of the abundances belies the real mixing proportions between these two components. The ultrarefractory-enriched patterns typically have much higher concentrations than do the ultrarefractory-depleted patterns. Perhaps, then, it is not surprising that the ultrarefractory-enriched pattern is so numerically underrepresented in CAIs.

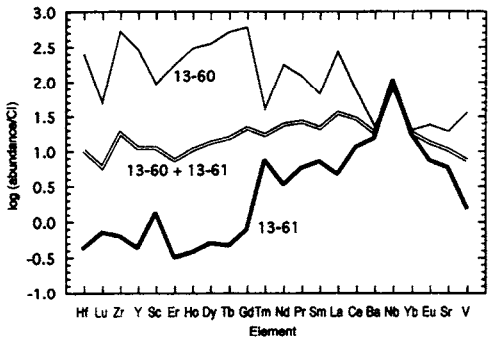

FIG. 17. Trace-element abundance plots for CAIs 13-60 and 13-61 ordered according to volatility. The hibonite patterns are more structured than Allende inclusions, probably because of magmatic fractionation of the REE during CAI crystallization. Nevertheless, summing the two patterns together reveals a relatively unfractionated pattern that indicates complementary volatile fractionations between these inclusions.

The refractory/lithophile-element fractionations require that different chemical components of the inventory be isolated from each other at different temperatures. For example, the ultrarefractory-enriched Murchison patterns reflect a higher-temperature component than the ultrarefractory-depleted pattern. Despite these distinct temperature fractionations, the mineralogy of the individual CAIs is decoupled from the trace-element fractionation pattern. As such there is no distinction mineralogically between an ultrarefractory-enriched SHIB and an ultrarefractory-depleted SHIB. Furthermore, the mineralogical associations as governed by major-element abundances in CAIs can be construed to cover a range of condensation temperatures. For example, Allende CAIs require condensation of the REE through to partial condensation of silicon (as melilite, pyroxene, and feldspar) to achieve the silicate-dominated mineralogy, whereas Murchison CAIs are commonly regarded as higher-temperature objects because of the lack of silicates and the presence of hibonite and perovskite. However, Group II–type patterns are found in both Allende and Murchison CAIs. Thus, the mineralogy of CAIs appears to be a regional function of the solar nebula and is not necessarily related to a single-stage condensation event that covers all elements. It is likely that the original REE-bearing condensates

were incorporated and dissolved into the proto-CAIs at a later stage.

Igneous fractionations are evident in CAIs through trace-element partitioning as well as major-element partitioning. This melting reflects secondary processing in the solar system. Most Murchison CAIs appear to have been molten, but there are fine-grained fluffy CAIs that have the physical characteristics of condensates. But real differences in trace-element chemistry between the textural condensates and the re-melted condensates do not exist. Evidently the condensation event imparts its own chemical memory on the material that constitutes the CAI. Re-melting the inclusion will simply repartition elements between solid and liquid. Yet at the temperatures required to melt these objects, it is still expected that some of the more volatile elements should be lost.

Such behavior is seen in HAL-type hibonite inclusions. HAL-type inclusions are characterized by isotopically heavy Ca and Ti (in terms of mass fractionation) as well as large Ce depletions (Ireland et al., 1992). These characteristics are consistent with thermal processing in an oxygen-rich environment, where Ce^{3+} is oxidized to the less refractory Ce^{4+}, which then evaporates from the object; schematically this process is represented by the net thermodynamic reaction

$$Ce_2O_3 \text{ (in solid solution)} + 0.5O_2 = 2CeO_2 \text{ (gas)}.$$

Similarly, the light isotopes of Ca and Ti are preferentially evaporated. Such behavior can be shown in experimental charges where less refractory materials are heated sufficiently to obtain hibonite-bearing residues (Ireland et al., 1992; Floss et al., 1996, 1998). However, other inclusions can show isotopic fractionation but do not show Ce depletions. This probably indicates that the effective oxygen fugacity was controlled by a combination of the H_2-rich nebular gas as well as by the more O_2-rich vapor evolved from the vaporizing CAIs. For instance, most CAIs contain reduced species as indicated by Ti^{3+}. However, the local environment may not be in equilibrium with the object being evaporated, and it is possible that sufficient time for equilibration might not exist if the time scale for melting is rapid. Furthermore, if inclusions become altered before re-melting, the nature of the evaporation event could be quite different.

It might be expected that FUN inclusions, being isotopically heavy in O, would have Ce depletions as well. Of the FUN inclusions, only HAL has a large Ce depletion, and it is more closely related to the group of hibonite inclusions. Other FUN inclusions apparently evaporated in a more reducing environment. But what is so special about FUN inclusions? Why is there a combination of a (relatively) large isotopic anomaly with mass fractionation? This association is not evident in Murchison CAIs with their much larger isotopic anomalies (in Ca and Ti at least). There is not a general progression in CAIs to compositions that are fractionated having larger non-linear anomalies. Furthermore PLACs and SHIBs were not necessarily the seeds for the larger CAIs from Allende. Very different sources for different types of inclusions probably are necessary.

Formation of CAIs

Time and place

CAIs are found commonly in carbonaceous chondrites, but also are found in many types of chondrites, including enstatite chondrites. The distinct characteristics of CAIs suggest that they have a common formation mechanism and perhaps the differences and commonalties among different types can tell us something about the actual mode of formation. However, there are innumerable problems in trying to ascertain what CAIs are really telling us about the early solar system. Were the inclusions formed during an early epoch when temperatures in the region were only then sufficiently high? Or, were CAIs formed continuously in a region through the early solar nebula, but could not escape later into the sampling region for chondritic parent bodies? We have a set of objects for which we have few constraints in terms of their original formation location and we have poor temporal resolution for timing of formation.

The entire population of CAIs is probably extremely biased, not only because of the dominance of a limited number of meteorites providing samples, but also because only those CAIs from a specific location and time period may have been entrained into the asteroidal parent bodies from which the source meteorites came. Other types of CAIs might have been formed at different stages, but these either fell into the Sun, or were swept up in the formation of the planets. Only the CAIs that ended up in the asteroid region have been preserved. In this case we must make a distinction between the CAI source region (the place where CAIs formed) and the CAI sampling region (that region of the source region from where the CAIs we

see have been derived). The sampling region may sample material from all over the source region, but it need not. For instance, might another CAI sampling region closer to the Sun have picked up a larger proportion of ultrarefractory-enriched CAIs?

CAIs contain phases such as perovskite with high U and low initial Pb concentrations, and thus U/Pb ages with high precision can be obtained. On an absolute time scale, CAIs provide the oldest U-Pb ages in the solar system at 4,566 Ma (Allègre et al., 1995). While CAIs provide a useful U-Pb chronometry, most other objects in chondrites (and especially chondrules) have low U and relatively high initial Pb, making precise measurements difficult. The next major time marker that is known to high precision in the U-Pb system is the age of angrites, achondrite meteorites formed during differentiation and melting of small planetary bodies. The angrite Angra dos Reis has been precisely dated at 4,557.8 ± 0.7 Ma (Lugmair and Galer, 1992). Thus the total time required for U-Pb closure of CAIs through to crystallization and closure of differentiated magmas on parent bodies is on the order of 8 Ma. But despite the high analytical precision available in the U-Pb system, it is still not sufficient to decipher possible age differences in different CAIs. And no other absolute chronometer (K[Ar]-Ar, Rb-Sr, Sm-Nd, Re-Os, etc) can provide the precision that is available from U-Pb.

Relative age differences can be established through the use of short-lived radionuclides such as ^{26}Al, ^{53}Mn, ^{107}Pd, ^{129}I, etc. (Wasserburg, 1985; Podosek and Swindle, 1988), but these have proved somewhat problematic in terms of obtaining agreement among these systems. While any system can give an internally consistent picture of the chronology, intercomparison shows discrepent time scales (Podosek and Swindle, 1988).

A major problem in interpreting early solar system chronology is the difficulty of obtaining age constraints on the formation of chondrules. The difficulty with chondrules is that they contain high abundances of Mg and Cr, limiting the usefulness of ^{26}Al and ^{53}Mn decay schemes, and other schemes such as K-Ar, I-Xe, etc. are obfuscated by low-temperature processes that remobilize the parent elements and disturb the systems. Recent work in the ^{26}Al system for phases having high Al/Mg (especially anorthite) suggests that chondrules may have formed within a million years or so of the CAIs (e.g., Hutcheon et al., 2000). Chondrules also require extremely high temperatures to melt, and so the extension of the CAIs forming epoch through chondrule formation is possibly a natural extension. All indications are that CAI formation took place over a short period of time and was quickly followed by chondrule formation.

But even though CAI formation took place over an apparently very short interval of time, the association of a number of diametrically opposed features cannot be accommodated in a simple single-stage event. REE fractionations apparently require a high-temperature condensation event for at least half of the CAIs having a Group II/ultrarefractory-depleted or ultrarefractory-enriched pattern, and yet there are no apparent mineralogical differences, especially in the Murchison inclusions. The chemistry of Allende inclusions suggests diverse oxidation states—in many cases, REE are not oxidized (no Ce anomaly), but siderophiles such as Mo and W have apparently been oxidized at some stage (Fegley and Palme, 1985), while the presence of Ti^{3+} indicates reducing conditions. These apparently contradictory indications suggest different processing for different components of the CAIs before final assembly of all the packages into proto-CAIs. Even then, the petrography of Allende (in particular) CAIs suggests that CAIs were melted and re-melted in the early solar system. What then are the minimum components required in the early solar system?

Condensates and residues

Condensation is required to form the Group II pattern. But the preservation of diverse isotopic anomalies is probably only consistent with the survival of refractory residues. We have previously suggested that the Group II pattern (and by extension other ultrarefractory-fractionated patterns) may be a result of condensation around another star and that this came into the solar system as a chemical memory (Fegley and Kornacki, 1984; Ireland, 1990). Although condensation around other stars is certainly occurring, it is probably unlikely that such a large fraction of solar system CAIs should have this pattern. We thus explore the consequences of having condensates and residues present as two end-members in the early solar system.

The specific characteristic of condensation is the ultrarefractory-REE fractionated pattern. Notwithstanding some notable exceptions, this pattern is typically accompanied by normal Ca and Ti isotopic compositions and ^{26}Al/^{27}Al of 5×10^{-5}, as is particularly evident in the Murchison SHIB inclusions.

We shall take these systematics as the attributes of the solar condensate.

Conversely, the presence of Ca and Ti isotopic anomalies is indicative of residual material that survived homogenization. In terms of Murchison inclusions, the PLACs are the carriers of these anomalies. Typically, these inclusions have Group III–type REE patterns with little or no excess ^{26}Mg associated with ^{26}Al decay.

It is unlikely that PLACs, SHIBs, or any other type of CAIs are pristine representatives of these two processes. However, these inclusions probably represent the best polarization of these components.

A longstanding issue with the PLACs is the absence of ^{26}Al effects, when the preservation of isotopic anomalies tends to suggest an early formation time. The prevalence of a maximum $^{26}Al/^{27}Al$ at 5×10^{-5} in the early solar system has been used as an argument that there was a uniform distribution of ^{26}Al and thence $^{26}Al/^{27}Al$ can be used as a chronometer (MacPherson et al., 1995). However, true uniformity of distribution would only be realized if there were no solid residues left in the early solar system—that is, all material in the solar system would need to be in the gas phase. As has been noted many times before, the preservation of diverse isotopic anomalies does not support this scenario. Any surviving refractory material with ^{27}Al cannot have a $^{26}Al/^{27}Al$ of 5×10^{-5}, and these objects cannot conform to a chronometric scheme based on ^{26}Al abundance.

The corollary to the presence of old ^{27}Al is that CAIs with $^{26}Al/^{27}Al$ of 5×10^{-5} must comprise Al that is almost entirely direct condensate of solar material. The canonical solar system value can only be obtained provided the CAIs formed early and the CAIs incorporated no old ^{27}Al. If CAIs formed over a short period of time (compared to the half-life), $^{26}Al/^{27}Al$ can be used as a tracer of the degree of ^{27}Al mixing. The PLAC hibonites incorporate residual material with diverse Ca and Ti isotopic compositions, but these objects are also likely to be rich in old ^{27}Al. It is thus the association of Ca and Ti isotopic anomalies with old ^{27}Al that yields the low apparent initial $^{26}Al/^{27}Al$ values, rather than the $^{26}Al/^{27}Al$ being a temporal indicator suggesting that PLAC hibonites are young.

Allende CAIs with near canonical $^{26}Al/^{27}Al$ should therefore contain little residue material and this is supported by their overall smaller Ti and Ca isotopic anomalies. FUN inclusions, with low $^{26}Al/^{27}Al$, have larger Ca and Ti anomalies, indicating a larger component of residue material. Thus the possible size of Ca and Ti isotopic anomalies is a natural consequence of the amount of residual material mixed in with a CAI. Still though, there is no particular indication as to why FUN inclusions should show large mass fractionation effects. In any case, the Allende CAIs are probably a poor set of inclusions to model early solar system behavior because of their size and the likely mixture of components present within them. The Ca-Ti compositions of Allende CAIs can be explained by a small amount of residue being incorporated into the proto-CAIs, which will not unduly upset the canonical $^{26}Al/^{27}Al$; a 20% addition of residue will only lower the $^{26}Al/^{27}Al$ from 5 to 4×10^{-5}, assuming the residue is dominated by ^{27}Al.

The association of Ca and Ti isotopic anomalies with low $^{26}Al/^{27}Al$ suggests that the presolar carriers responsible for these characteristics were aluminous and possibly even hibonite itself. There is no *a priori* expectation of a distinct trace-element signature for the residues. That is, any REE abundance might be possible depending on the r- to s-process abundance ratio as well as mixtures in the precursors. Isotopic compositions of REE would be illuminating in this respect, but we can already note that Zr isotopes in hibonite 13-13, which has a 27% excess of ^{50}Ti, are normal (Ireland, 1994), and therefore a local origin for the REE cannot be ruled out. Indeed the Group III pattern is the most common for PLACs. This pattern indicates the more refractory REE are in their solar abundances, and they may therefore be unassociated with the carriers of the Ca and Ti isotopic anomalies. If the PLAC precursor was mixed with material that had solar relative abundances of the REE, a Group III pattern would be produced simply by the melting of the proto CAIs and thence evaporation of Eu and Yb. These observations suggest that the residues themselves have little in the way of REE and that the PLAC REE systematics were established in the solar nebula.

The problem with oxygen

Large oxygen isotopic anomalies are a characteristic feature of CAIs, yet despite widely different Ca and Ti isotopic compositions, initial ^{26}Al abundance, and REE patterns, ^{16}O excesses in CAIs of several percent are the norm. In comparison, presolar oxides (including corundum and hibonite) have diverse oxygen isotopic compositions with highly anomalous $^{17}O/^{16}O$ and $^{18}O/^{16}O$ ratios (Hutcheon et al., 1994; Nittler et al., 1997; Choi et al., 1999).

Furthermore, both PLACs (dominantly residues) and SHIBs (condensate), as well as Allende CAIs have the same oxygen isotope compositions, typically with an enrichment in ^{16}O of 50‰ relative to terrestrial oxygen. Even the most anomalous hibonite, Murchison inclusion BB-5, only shows an enrichment of 70‰ (Fahey et al. 1987).

The lack of any diversity in oxygen isotopic compositions is not consistent with the retention of original oxygen in the CAI-precursor residues, if the compositions of the presolar oxides are indicative of the possible range in compositions that existed. Clayton and Mayeda (1984) argued that the ^{16}O enrichment is a signature of solids in the solar nebula while normal O was in the gas phase, but this reflects possibly only the final stage in CAI formation. The lack of any diversity in O isotopic compositions in CAIs suggests that CAI precursors must have equilibrated with a ^{16}O-rich gas in the solar nebula, thereby erasing their original compositions. In order to homogenize the precursors, the ^{16}O-enriched gas must have been pervasive throughout the CAI-forming region, at least in the initial stages. One potential source is the evaporation of a ^{16}O-enriched phase with a low vaporization temperature, although there is no indication for the preservation of this phase in meteorites. Alternatively, a ^{16}O-enriched reservoir may have been produced by chemical processing of material in the accretion disk (Thiemens, 1996). Nevertheless, the oxygen isotopic systematics tend to suggest a progressive change from the extreme ^{16}O enrichment of ~70‰ found in Murchison CAIs, through 50‰ for Allende CAIs, and to 20‰ and less for chondrules (Leshin et al., 1997, 2000). The formation of planetary bodies evidently took place with O-isotope heterogeneity, as indicated by differing compositions of meteorite parent bodies, Earth, and Moon, but with compositions closer to what we would regard as normal. CAI O-isotope systematics do not reflect the protoliths or precursors in the solar nebula and so polarization of systematics is not be expected between condensates and residues.

Processes and mechanisms

The existence of CAIs attests to high temperatures being attained in the solar nebula. But the CAI systematics described above cannot be placed into a single-stage model of formation that is consistent with the condensation sequence and the preservation of isotopic anomalies. Both condensates and residues are required and both experienced high temperatures. In the simplest scenario, partial condensation can be invoked to produce the Group II REE fractionation, whereas isotopic anomalies are preserved in refractory residues such as Murchison PLAC CAIs. But the systematics are more complicated than this.

It appears that condensation of the refractory trace elements must be decoupled from the major-element components Ca, Al, Ti, Si, and Mg. The evidence for this is the lack of correlation between REE and lithophile patterns and bulk composition in Allende CAIs, the lack of correlation between siderophile patterns and bulk composition in Allende CAIs, and the petrographic similarity of ultrarefractory-enriched and ultrarefractory-depleted CAIs in Murchison. In Allende CAIs, it is possible that all the major elements condensed with the Group II pattern because of the possible continuity of condensation from light REE through to Si and Mg. However, in Murchison CAIs, it would not be expected that an ultrarefractory residue could have the same major-element composition as the condensate (Group II). At the very least, elemental volatility-controlled fractionation of Ca, Ti, and Al relative to Mg and Si would occur with the former elements present in the ultrarefractory-enriched CAIs, and the latter with the Group II condensates. This is clearly not the case.

Allende CAIs can simply form from a mix of condensates to produce the range of trace element patterns observed. The ultrarefractory trace elements may have mixed in with Group II condensate to reform a flat abundance pattern for the refractory REE (which is the Group III characteristic), or with fully chondritic relative abundances (Group I). However, the ultrarefractory component was not preserved in the Allende CAI formation area. This further suggests a lack of association of the major elements Al, Ca, and Ti, which themselves are highly refractory, with the REE condensation sequence, at least insofar as the required chemical inventory for Allende CAIs is concerned. In the Murchison SHIB CAI-forming zone, pockets of ultrarefractory-enriched and ultrarefractory-depleted REE are preserved. Eventually the REE components mixed with very similar proportions of the major elements to form SHIB CAIs with similar bulk compositions of major elements (i.e., dominated by spinel-hibonite).

Allende CAIs are dominated by melilite and pyroxene (both silicates), whereas the dominant mineralogy in SHIBs is oxide: spinel-hibonite-per-

ovskite. There is no Si-bearing phase in SHIBs despite Si condensing in melilite at a higher temperature than spinel (Fig. 1). Basically, these inclusions represent a similar problem as Group II patterns do for REE, only in reverse. SHIBs preserve the high-temperature (REE) component in a lower-temperature matrix (spinel), and the intermediary silicate is missing. In the context of condensation, this would require that the melilite failed to condense before Mg came out as spinel, and the CAI was isolated from the gas prior to forsterite/diopside condensation. Alternatively, condensation of spinel may have been achieved in a Si-depleted region of the solar nebula that could have formed by vaporization of chondritic material, separation of the vapor and residue, and reaction of the Mg-rich vapor with the Al-rich residue to form the bulk compositions observed. Conversely, the evaporation experiments of Hashimoto (1983) indicate that Mg was more volatile than Si, and so evaporation and recondensation of spinel is possible.

CAIs experienced multiple reheating episodes, as indicated by textural relationships. However, most subsequent events had to be at temperatures sufficient to melt the CAIs, but not enough to cause complete evaporation of Mg. However, even at these temperatures Eu and Yb will be evaporated and recondensed, allowing a variety of REE patterns (such as Group I, III, V, and VI). The FUN inclusions may represent an early phase of CAIs where isotopic heterogeneities were more widespread and heating to higher temperatures after formation was possible. Even then, however, all elements cannot experience Rayleigh mass fractionation at the same time. For instance, Mg will be totally evaporated from the residue before Ti begins to evaporate.

Thus CAIs represent the culmination of many processes that provide inconsistent indications to the formation environment in the solar nebula. The lack of systematics in Allende CAIs is therefore not surprising. But the systematic behavior of Murchison CAIs in general allows the extraction of some details of the individual processes.

The solar nebula

From our present knowledge of the solar system, and inferences drawn from observations of other young stellar systems, we can set up some boundary conditions and see what the implications are for formation of CAIs. The Sun is now sufficiently hot to hold all elements in a gaseous form. It is likely that once ignited, the early sun could do the same. At the outer edges of the solar system, comets and the survival of presolar materials in meteorites indicate that not all presolar material was held in the gaseous phase (Fegley, 1999). In between these extremes, there is partial to complete volatilization, depending on the volatility of individual chemical species. This is also the condensation line for vaporized material in a cooling nebula. The condensation line is not a constant for the solar nebula, but depends on a number of parameters such as in-fall rate, opacity, etc.

A description of the formation of CAIs requires an understanding of the evolution of the solar nebula, which comprises the transformation of a molecular cloud into a proto-solar system. With the direct observation of proto-planetary systems with the Hubble Space Telescope, such discussion can be placed into a context that has not previously been possible. Cameron (1995) divided the evolution of the solar system into four stages, as summarized below:

Stage 1. Molecular cloud collapse. In-falling material produces the nebular disk from the molecular cloud core over a time period of a few times 10^5 years. Initially the disk mass is greater than the mass of the proto-Sun, but ultimately most matter is captured by the Sun.

Stage 2. Disk dissipation. The Sun forms at a rate of 2×10^{-5} solar masses per year—i.e., a total time of 50,000 years. Matter falling onto the accretion disk is transported to the proto-Sun—i.e., matter is transported inward, but angular momentum is transported outward through the geometrically thin disk. The major transport mechanisms are spiral density waves, disk-driven bipolar outflows, and the Balbus-Hawley magnetic instability.

Stage 3. Terminal accumulation of the Sun. The final accumulation lasts for 1 to 2 million years, with an accumulation rate decreasing from 10^{-7} to 10^{-8} solar masses per year. The proto-Sun becomes a classical T-Tauri in this phase. Planetary accretion occurs.

Stage 4. Loss of nebular gas. The Sun becomes a weak line T-Tauri star in a time period covering 3–30 million years. Material is no longer being accreted from the disk, and the T-Tauri wind removes gas from the inner nebula.

Clearly, the highest temperatures in the solar nebula will be obtained with the highest in-fall rates and these occur in the earliest stages (predominantly stage 2) of nebula evolution. The entire span of Stages 1 and 2 is only on the order of 150,000 years, which is entirely consistent with the $^{26}Al/^{27}Al$

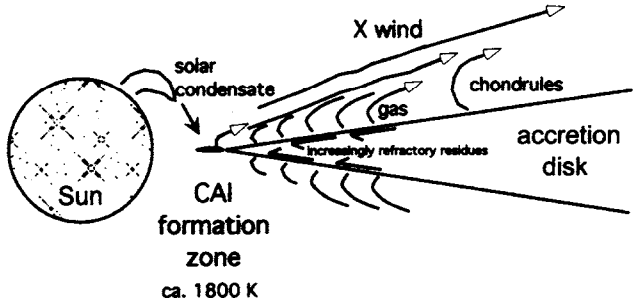

FIG. 18. Schematic view of the CAI formation process in the early solar system. CAIs are formed from a mixture of solar condensate and refractory residue falling in through the accretion disk. The solar condensate is responsible for the refractory lithophile fractionations typically observed in CAIs. The residues carry isotopic anomalies in refractory elements. CAIs are melted and transported to the planetary reaches of the solar system by protostellar winds such as the X-wind postulated by Shu et al. (1996).

systematics of the SHIB inclusions. However, chondrule formation appears to occur at least one half-life after CAI formation, which is of the order of 750,000 years, and so the quandary of the mechanism of chondrule formation in the solar system remains.

The most likely location for the high temperatures required for CAI formation is close to the Sun and close to the mid-plane of the accretion disk of the solar nebula. Woolum and Cassen (1999) have examined T-Tauri stars and found temperatures at the mid-plane only exceed 1500 K at distances typically less than 0.5 a.u. Temperatures at earlier times (1 m.y. earlier) could have been substantially higher, allowing volatilization of silicates. But CAI temperatures require volatilization of REE, and this is likely to occur only in close proximity to the Sun.

In fact, it is likely that the only place where REE can exist entirely in the gas phase is within the Sun. Then condensates must be samples of the Sun that have been ejected to the CAI formation region. Such outflow could be provided by winds, flares, or jets of material from the early Sun. Progressive condensation of the gas to smokes or small grains (Nuth and Dodd, 1983) will occur as the outflow progresses, and so a mechanism for elemental fractionation exists in this scenario. Thus, the ultrarefractory carriers condense out closest to the Sun and this can be most readily re-accreted back to the Sun. In this case, a Group II pattern is to be expected as more common than the ultrarefractory-enriched pattern. These REE components are mixed in the CAI-forming region to greater or lesser degrees. Aluminium condensing from the Sun has the canonical $^{26}Al/^{27}Al$ ratio, and the oxygen isotopic composition in the gas of the condensation region is ^{16}O enriched. Furthermore, this oxygen largely equilibrates with infalling refractory residues, wiping out original O isotopic compositions. It remains an unknown as to whether this O composition reflects the nebula, the Sun, or the chemical processing in the region (Wiens et al., 1999). Condensate material can be accreted onto residues and form CAIs such as PLACs, which retain isotopic diversity in the refractory elements Ca and Ti, and retain old ^{27}Al.

The formation of CAIs must occur close to the Sun simply to attain the temperatures necessary to melt CAIs (~1800–2000 K). Once formed, these CAIs must be ejected out of the inner region to the asteroid zone, where they were eventually collected in chondritic materials. However, CAIs also could experience multiple heating events if the ejection mechanism is not very efficient and some CAIs can fall out and remain close to the CAI-forming region while others are transported away to the asteroid belt.

Such a scenario is very much in accord with the X-wind models of Shu and colleagues (Shu et al., 1996; Lee et al., 1998; Shang et al., 2000). In their model, CAIs form close to the Sun at ~0.06 AU, and are then thrown out to planetary distances from a bipolar outflow. The CAIs (and chondrules) are picked up by the aerodynamic drag of a magneto-centrifugally driven wind. The source of material for CAIs and chondrules is the infalling accretion disk. Proto-CAIs and -chondrules experience flash heating as they are taken out of the shielded disk and into the sunlight. The general model is illustrated in Figure 18.

There remain several unsatisfactory corollaries to this model. If volatiles are driven off the rapidly melting objects, substantial isotopic mass fractionation should be present in the transformation from an aggregate that is near-chondritic to refractory. The exposure to energetic particles can produce short-lived radionuclides, although not in direct proportion to observations.

However, the presence of bipolar jets in young stellar objects is now an essential part of the evolution of a star on to the main sequence. This provides the source of energy for transport of CAIs from close to the Sun to the outer reaches of the solar system where they can be entrained in asteroidal bodies. In view of the chemical and isotopic systematics reviewed here, close proximity to the Sun is essential for the mixing of solar condensate with refractory residues that survive transport into the solar system.

Synthesis

CAIs represent the earliest formed objects in the solar system. They preserve chemical and isotopic features not found in any other objects and are a window into high-temperature processes in the solar system.

Trace-element patterns with ultrarefractory depletions and enrichments require a condensation event to fractionate these elements. The only place compatible with such extreme temperatures is the Sun itself. Condensates from solar gas eruptions or outflows are then mixed with proto-CAIs.

The ^{16}O-enriched signature in CAIs might be a response to the extreme chemical processing taking place in the leading edge of the accretion disk. There is no correlation between O isotopic anomalies and anomalies in other elements, suggesting that any original nucleosynthetic anomalies have been wiped out.

Isotopic anomalies in refractory elements (especially Ca and Ti) are preserved in refractory residues.

Short-lived radionuclides may be produced by high-energy particle reactions, but the abundance of ^{26}Al and its correlation with other chemical and isotopic characteristics suggests that it is indeed a nucleosynthetic input. The canonical $^{26}Al/^{27}Al$ of the early solar system can only be obtained for condensates largely free of aluminous (i.e., old ^{27}Al) residues.

The final chemical and isotopic systematics cannot be described in terms of any single process, but require the superposition of condensation of solar gas, the preservation of isotopic anomalies in refractory residues, and the melting of mixtures of these components into the objects we now see. CAIs remain enigmatic, but the observed correlations in chemistry and isotopics, and better insights into the astrophysical environment, offer us the possibility of a better understanding of the chemistry of the early solar system.

Acknowledgments

This work was supported by NASA Cosmochemistry Program (Grant NAG5-7609 to TRI) and the NASA Origins of Solar System Program (Grant NAG5-4323 to BF). Kevin McKeegan and Sasha Krot kindly provided reviews that were of great use in the preparation of this manuscript.

REFERENCES

Allègre, C. J., Gèrard, M., and Göpel, C., 1995, The age of the Earth: Geochim. et Cosmochim. Acta, v. 59, p. 1445–1456.

Allen, J. M., Grossman, L., Davis, A. M., and Hutcheon, I. D., 1978, Mineralogy, textures, and mode of formation of a hibonite-bearing Allende inclusion: Proc. Lunar Planet. Sci. Conf., v. 9, p. 1209–1233.

Amari, S., Hoppe, P., Zinner, E., and Lewis, R. S., 1992, Interstellar SiC with unusual SiC compositions: Grains from a supernova?: Astrophys. Jour. (Lett.), v. 394, p. L43–L46.

Bar-Matthews, M., Hutcheon, I. D., MacPherson, G. J., and Grossman, L., 1982, A corundum-rich inclusion in the Murchison carbonaceous chondrite: Geochim. et Cosmochim. Acta. v. 46, p. 31–41.

Beckett, J. R., and Stolper, E., 1994, The stability of hibonite, melilite and other aluminous phases in silicate melts: Implications for the origin of hibonite-bearing inclusions from carbonaceous chondrites: Meteoritics, v. 29, p. 41–65.

Birck, J. L., and Allègre, C. J., 1984, Chromium isotopic anomalies in Allende refractory inclusions: Geophys Res. Lett., v. 11, p. 943–946.

Birck, J. L., and Lugmair, G. W., 1988, Nickel and chromium isotopes in Allende inclusions: Earth Planet. Sci. Lett., v. 90, p. 131–143.

Blander, M., and Fuchs, L. H., 1975, Calcium-aluminum-rich inclusions in the Allende meteorite: Evidence for a liquid origin: Geochim. et Cosmochim. Acta, v. 39, p. 1605–1619.

Boynton, W. V., 1975, Fractionation in the solar nebula: Condensation of yttrium and the rare earth elements: Geochim. et Cosmochim. Acta, v. 39, p. 569–584.

Boynton, W. V., Frazier, R. M., and Macdougall, J. D., 1980, Identification of an ultrarefractory component in the Murchison meteorite: Lunar Planet. Sci., v. XI, p. 103–105.

Cameron, A. G. W., 1962, The formation of the Sun and planets: Icarus, v. 1, p. 13–69.

_____, 1995, The first ten million years in the solar nebula: Meteoritics, v. 30, p. 133–161.

Cameron, A. G. W., and Truran, J. W., 1977, The supernova trigger for formation of the solar system: Icarus, v. 30, p. 447–461.

Choi, B.-G., Wasserburg, G. J., and Huss, G. R., 1999, Circumstellar hibonite and corundum and nucleosynthesis in asymptotic giant branch stars: Astrophys. Jour. (Lett.), v. 522, p. L133–L136.

Clark, R. S., Jr., Jarosewich, E., Mason, B., Nelen, J., Gomez, M., and Hyde, J. R., 1970, The Allende, Mexico, meteorite shower: Smithson. Contrib. Earth Sci., v. 5, p. 1–53.

Clayton, D. D., 1982, Cosmic chemical memeory: A new astronomy: Jour. Roy. Astron. Soc., v. 23, p. 174–212.

Clayton, D. D., and Leising, M., 1987, ^{26}Al in the interstellar medium: Phys. Rept., v. 144, p. 1–50.

Clayton, R. N., Grossman, L., and Mayeda, T. K., 1973, A component of primitive nuclear composition in carbonceous chondrites: Science, v. 182, p. 485–488.

Clayton, R. N., Hinton, R. W., and Davis, A. M., 1988, Isotopic variations in the rock-forming elements in meteorites: Phil. Trans. Roy. Soc. Lond., v. A325, p. 483–501.

Clayton, R. N., and Mayeda, T. K., 1977, Correlated oxygen and magnesium isotope anomalies in Allende inclusions, I: Geophys. Res. Lett., v. 4, p. 295–298.

_____, 1984, The oxygen isotope record in Murchison and other carbonaccous chondrites: Earth Planet. Sci. Lett., v. 67, p. 151–161.

Clayton, R. N., Onuma, N., Grossman, L., and Mayeda, T. K., 1977, Distribution of the presolar component in Allende and other carbonaceous chondrites: Earth Planet. Sci. Lett., v. 34, p. 209–224.

Davis, A. M., and Grossman, L., 1979, Condensation and fractionation of rare earths in the solar nebula: Geochim. et Cosmochim. Acta, v. 43, p. 1611–1632.

Fahey, A. J., Goswami, J. D., McKeegan, K. D., and Zinner, E., 1987, ^{16}O excesses in Murchison and Murray hibonites: A case against a late supernova injection origin of isotopic anomalies in O, Mg, Ca, and Ti: Astrophys. Jour.(Lett.), v. 323, p. L91–L95.

Fegley, B., Jr., 1999, Chemical and physical processing of presolar materials in the solar nebula and the implications for preservation of presolar material in comets: Space Sci. Rev., v. 90, p. 239–252.

Fegley, B., Jr., and Ireland, T. R., 1991, Chemistry of the rare earth elements in the solar nebula: Eur. Jour. Solid State Inorg. Chem., v. 28, p. 335–346.

Fegley, B., Jr., and Kornacki, A. S., 1984, The geochemical behavior of refractory noble metals and lithophile trace elements in refractory inclusions in carbonaceous chondrites: Earth Planet. Sci. Lett., v. 68, p. 181–197.

Fegley, B., Jr., and Palme, H., 1985, Evidence for oxidizing conditions in the solar nebula from Mo and W depletions in refractory inclusions in carbonaceous chondrites: Earth Planet. Sci. Lett., v. 72, p. 311–326.

Floss, C., El Goresy, E., Zinner, E., Kransel, G., Rammansee, W., and Palme, H., 1996, Elemental and isotopic fractionations produced through evaporation of the Allende CV3 chondrite: Implications for the origin of HAL-type hibonite inclusions: Geochim. et Cosmochim. Acta, v. 60, p. 1975–1997.

Floss, C., El Goresy, E., Zinner, E., Palme, H., Weckwerth, G., and Rammansee, W., 1998, Corundum-bearing residues produced through the evaporation of natural and synthetic hibonite: Meteoritics& Planet. Sci., v. 33, p. 191–206.

Fuchs, L.H., Olsen, E., and Jensen, K. J., 1973, Mineralogy, mineral chemistry, and composition of the Murchison (C2) meteorite: Smithson. Contrib. Earth Sci., v. 10, p. 1–39.

Gray, C. M., and Compston, W., 1974, Excess ^{26}Mg in the Allende meteorite: Nature, v. 251, p. 495–497.

Grossman, L., 1972, Condensation in the primitive solar nebula: Geochim. et Cosmochim. Acta, v. 36, p. 597–619.

Grossman, L., 1975, Petrography and mineral chemistry of Ca-rich inclusions in the Allende meteorite: Geochim. et Cosmochim. Acta, v. 39, p. 433–454.

_____, 1980, Refractory inclusions in the Allende meteorite: Ann. Rev. Earth Planet. Sci., v. 8, p. 559–608.

Hartmann, D., Woosley, S. E., and El Eid, M. F., 1985, Nucleosynthesis in neutron-rich supernova ejecta: Astrophys. Jour. (Lett.), v. 297, p. 837–845.

Hashimoto, A., 1983, Evaporation metamorphism in the early solar nebula—evaporation experiments on the melt FeO-MgO-SiO_2-CaO-Al_2O_3 and chemical fractionations of primitive materials: Geochem. Jour., v. 17, p. 111–145.

Haskin, L. A., Helmke, P. A., Paster, T. P., and Allen, R. O., 1971, Rare earths in meteoritic, terrestrial, and lunar matter, *in* Activation anal. geochem. cosmochem.: Oslo, Universitetsforlaget, Proc. NATO Advanced Study Institute, p. 201–218.

Heydegger, H. R., Foster, J. J., and Compston, W., 1979, Evidence of a new isotopic anomaly from titanium isotopic ratios in meteoric materials: Nature, v. 278, p. 704–707.

Hinton, R. W., Davis, A. M., and Scatena-Wachel, D. E., 1987, Large negative ^{50}Ti anomalies in refractory inclusions from the Murchison carbonaceous chondrite—Evidence for incomplete mixing of neutron-rich supernova ejecta into the solar system: Astrophys. Jour. (Lett.), v. 313, p. 400–428.

Hinton, R. W., Davis A. M., Scatena-Wachel, D. E., Grossman, L., and Draus, R. J., 1988, A chemical and isoto-

pic study of hibonite-rich refractory inclusions in primitive meteorites: Geochim. et Cosmochim. Acta, v. 52, p. 2573–2598.

Hutcheon, I. D., Huss, G. R., Fahey, A. J., and Wasserburg, G. J., 1994, Extreme ^{26}Mg and ^{17}O enrichments in an Orgueil corundum: Identification of a presolar oxide grain: Astrophys. Jour. (Lett.), v. 425, p. L97–L100.

Hutcheon, I. D., Krot, A. N., and Ulyanov, A. A., 2000, ^{26}Al in anorthite-rich chondrules in primitive carbonaceous chondrites: Evidence chondrules post-date CAIs [abs.]: Lunar Planet Sci., v. XXXI, abs. no. 1869.

Hutcheon, I. D., Steele, I. M., Wachel, D. E. S., Macdougall, J. D., and Phinney, D., 1983, Extreme Mg fractionation and evidence of Ti isotopic variations in Murchison refractory inclusions: Lunar Planet. Sci., v. XIV, p. 339–340.

Ihinger, P. D., and Stolper, E., 1986, The color of meteoritic hibonite: an indicator of oxygen fugacity. Earth Planet. Sci. Lett., v. 78, p. 67–79.

Ireland, T. R., 1988, Correlated morphological, chemical and isotopic characteristics of hibonites from the Murchison carbonaceous chondrite: Geochim. et Cosmochim. Acta, v. 52, p. 2827–2839.

_____, 1990, Presolar isotopic and chemical signatures in hibonite-bearing refractory inclusions from the Murchison carbonaceous chondrite: Geochim. et Cosmochim. Acta, v. 54, p. 3219–3237.

_____, 1994, Isotopically normal zirconium in Murchison hibonite 13-13: Implications for a link between e and r processes: Astrophys. Jour. (Lett.), v. 434, p. L79–L81.

_____, 1995, Ion microprobe mass spectrometry: Techniques and applications in cosmochemistry, geochemistry, and geochronology, *in* Hyman, M., and Rowe, M., Advances in analytical geochemistry, v. 2: Greenwich, UK, JAI Press, p. 1–118.

Ireland, T. R., Fahey, A. J., and Zinner, E. K., 1988, Trace-element abundances in hibonites from the Murchison carbonaceous chondrite: Constraints on high-temperature processes in the solar nebula: Geochim. et Cosmochim. Acta, v. 52, p. 2841–2854.

_____, 1991, Hibonite-bearing microspherules: A new type of refractory inclusion with large isotopic anomalies: Geochim. et Cosmochim. Acta, v. 55, p. 367–379.

Ireland, T. R., Zinner, E. K., Fahey, A. J., and Esat, T. M., 1992, Evidence for distillation in the formation of HAL and related hibonite inclusions: Geochim. et Cosmochim. Acta, v. 56, p. 2503–2520.

Jungck, M. H. A., Shimamura, T., and Lugmair, G. W., 1984, Ca isotope variations in Allende: Geochim. et Cosmochim. Acta, v. 48, p. 2651–2658.

Kimura, M., El Goresy, A., Palme, H., and Zinner, E., 1993, Ca-, Al-rich inclusions in the unique chondrite ALH85085: Petrology, chemistry, and isotopic compositions: Geochim. et Cosmochim. Acta, v. 57, p. 2329–2359.

Kornacki, A. S., and Fegley, B., Jr., 1986, The abundance and relative volatility of refractory trace elements in Allende Ca, Al-rich inclusions: Implications for chemical and physical processing in the solar nebula: Earth Planet. Sci. Lett., v. 79, p. 217–234.

Lauretta, D. S., and Lodders, K., 1997, The cosmochemical behavior of beryllium and boron: Earth Planet. Sci. Lett., v. 146, p. 315–327.

Lee, T., 1988, Isotopic anomalies, *in* Kerrdige, J. F., and Matthews, M. S., eds., Meteorites and the early solar system: Tucson, Univ. of Arizona Press, p. 1063–1089.

Lee, T., Mayeda, T. K., and Clayton, R. N., 1980, Oxygen isotopic anomalies in Allende inclusion HAL: Geophys. Res. Lett., v. 7, p. 493–496.

Lee, T., and Papanastassiou, D. A., 1974, Mg isotopic anomalies in the Allende meteorite and correlation with O and Sr effects: Geophys. Res. Lett., v. 1, p. 225–228.

Lee, T., Papanastassiou, D. A., and Wasserburg, G. J., 1977, Aluminium-26 in the early solar system: Fossil or fuel?: Astrophys. Jour.(Lett.), v. 211, p. L107–L110.

Lee, T., Shu, F. H., Shang, H., Glassgold, A., and Rehm, K. E., 1998, Protostellar cosmic rays and extinct radioactivities in meteorites: Astrophys. Jour. (Lett.), v. 506, p. 898–912.

Leshin, L. A., Rubin, A. E., and McKeegan, K. D., 1997, The oxygen isotopic composition of olivine and pyroxene from CI chondrites: Geochim. et Cosmochim. Acta, v. 61, p. 835–845.

Leshin, L. A., McKeegan, K. D., and Benedix, G. K., 2000, Oxygen isotope geochemistry of olivine from carbonaceous chondrites [abs.]: Lunar Planet Sci., v. XXXI, abstract No. 1918.

Lodders, K., and Fegley, B., Jr., 1993, Lanthanide and actinide chemistry at high C/O ratios in the solar nebula: Earth Planet. Sci. Lett., v. 117, p. 125–145.

Loss, R. D., and Lugmair, G. W., 1990, Zinc isotope anomalies in the Allende meteorite: Astrophys. Jour. (Lett.), v. 228, p. L93–L98.

Lugmair, G. W., and Galer, S. J. G., 1992, Age and isotopic relationship among the angrites Lewis Cliff 86010 and Angra Dos Reis: Geochim. et Cosmochim. Acta, v. 56, p. 1673–1694.

MacPherson, G. J., and Davis, A. M., 1994, Refractory inclusions in the prototypical CM chondrite, Mighei: Geochim. et Cosmochim. Acta, v. 58, p. 5599–5625.

MacPherson, G. J., Davis, A. M., and Zinner, E. K., 1995, The distribution of aluminum-26 in the early solar system—a reappraisal: Meteoritics, v. 30, p. 365–386.

MacPherson, G. J., Grossman, L., Hashimoto, A., Bar-Matthews, M., and Tanaka, T., 1984, Petrographic studies of refractory inclusions from the Murchison meteorite: Jour. Geophys. Res. B., v. 89 (suppl.), p. C299–C312.

MacPherson, G. J., Wark, D. A., and Armstrong J. T., 1988, Primitive material surviving in chondrites: Refractory inclusions, *in* Kerrdige, J. F., and Mat-

thews, M. S., eds., Meteorites and the early solar system: Tucson, Univ. of Arizona Press, p. 746–807.

Marvin, U. B., Wood, J. A., and Dickey, J. S., Jr., 1970, Ca-Al-rich phases in the Allende meteorite: Earth Planet. Sci. Lett., v. 7, p. 346–350.

Mason, B., and Taylor, S. R., 1982, Inclusions in the Allende meteorite: Smithson. Contrib. Earth Sci., v. 25, p. 1–39.

McKeegan, K. D., Chaussidon, M., and Robert, F., 2000, Incorporation of short-lived ^{10}Be in a calcium-aluminum-rich inclusion from the Allende Meteorite: Science, v. 289, p. 1334–1337.

McKeegan, K. D., Leshin, L., Russell, S. S., and MacPherson, G. J., 1998, Oxygen isotopic abundances in calcium-aluminum-rich inclusions from ordinary chondrites: Implications for nebular heterogeneity: Science, v. 280, p. 414–418.

Meyer, B. S., Krishnan, T. D., and Clayton, D. D., 1996, ^{48}Ca production in matter expanding from high temperature and density: Astrophys. Jour. (Lett.), v. 462, p. 825–838.

Niederer, F. R., Papanastassiou, D., and Wasserburg, G. J., 1980, Endemic isotopic anomalies in titanium: Astrophys. Jour. (Lett.), v. 240, p. L73–L77.

_____, 1985, Absolute isotopic abundances of Ti in meteorites: Geochim. et Cosmochim. Acta, v. 49, p. 835–851.

Niemeyer, S., and Lugmair, G. W., 1981, Ubiquitous isotopic anomalies in Ti from normal Allende inclusions: Earth Planet. Sci. Lett., v. 53, p. 211–225.

Nittler, L. R., Alexander, C. M. O'D., Gao, X., Walker, R. M., and Zinner, E., 1997, Stellar sapphires: The properties and origins of presolar Al_2O_3 in meteorites: Astrophys. Jour. (Lett.), v. 483, p. 475–495.

Nuth, J., and Donn, B., 1983, Nucleation theory is not applicable to the condensation of refractory grains in the primitive solar nebula: Lunar Planet. Sci., v. XIV, p. 570–571.

Palme, H., Wlotzka, F., Nagel, K., and El Goresy, A., 1982, An ultra-refractory inclusion from the Ornans carbonaceous chondrite: Earth Planet. Sci. Lett., v. 61, p. 1–12.

Podosek, F. A., and Swindle, T. D., 1988, Extinct radionuclides, *in* Kerrdige, J. F., and Matthews, M. S., eds., Meteorites and the early solar system: Tucson, Univ. of Arizona Press, p. 1093–1113.

Reynolds, J. H., 1967, Isotopic abundance anomalies in the solar system: Ann. Rev. Nucl. Phys., v. 17, p. 253–316.

Russell, S. S., Huss, G. R., Fahey, A. J., Greenwood, R. C., Hutchison, R., and Wasserburg, G. J., 1998, An isotopic and petrologic study of calcium-aluminum-rich inclusions from CO3 meteorites: Geochim. et Cosmochim. Acta, v. 62, p. 689–714.

Ryerson, F. J., and McKeegan, K. D., 1994, Determination of oxygen self-diffusion in åkermanite, anorthite, diopside, and spinel: Implications for oxygen isotopic anomalies and the thermal histories of Ca-Al-rich inclusions: Geochim. et Cosmochim. Acta, v. 58, p. 3713–3734.

Shang, H., Shu, F. H., Lee, T., and Glassgold, A. E., 2000, Protostellar winds and chondritic meteorites: Space Sci. Rev., v. 92, p. 153–176.

Shu, F., Shang, H., and Lee, T., 1996, Toward an astrophysical theory of chondrites: Science, v. 271, p. 1545–1552.

Simon, S. B., Davis, A. M., and Grossman, L., 1996, A unique ultrarefractory inclusion from the Murchison meteorite: Meteorit. Planet. Sci., v. 31, p. 106–115.

_____, 1998, Formation of an unusual compact Type A refractory inclusion from Allende: Meteorit. Planet. Sci., v. 33, p. 115–126.

Simon, S. B., Davis, A. M., Grossman, L., and Zinner, E. K., 1998, Origin of hibonite-pyroxene spherules found in carbonaceous chondrites: Meteorit. & Planet. Sci., v. 33, p. 411–424.

Srinivasan, G., Sahijpal, S., Ulyanov, A. A., and Goswami, J. N., 1996, Ion microprobe studies of Efremovka CAIs: II. Potassium isotope composition and ^{41}K in the early solar system: Geochim. et Cosmochim. Acta, v. 60, p. 1823–1835.

Srinivasan, G., Ulyanov, A. A., Hutcheon, I. D., and Goswami, J. N., 1994, Excess ^{41}K in the early solar system: Astrophys. Jour. (Lett.), v. 431, p. L67–L70.

Suess, H. E., 1965, Chemical evidence bearing on the origin of the solar system: Ann. Rev. Astron. Astrophys., v. 3, p. 217–234.

Sylvester, P. J., Grossman, L., and MacPherson, G. J., 1992, Refractory inclusions with unusual chemical compositions from the Vigarano carbonaceous chondrite: Geochim. et Cosmochim. Acta, v. 56, p. 1343–1363.

Sylvester, P. J., Simon, S. B., and Grossman, L., 1993, Refractory inclusions from the Leoville, Efremovka, and Vigarano C3V chondrites: Major element differences between Types A and B, and extraordinary refractory siderophile element compositions: Geochim. et Cosmochim. Acta, v. 57, p. 3763–3784.

Thiemens, M. H., 1996, Mass-independent isotopic effects in chondrites: The role of chemical processes, *in* Hewins, R., Jones, R., and Scott, E., eds., Chondrules and the protoplanetary disk: Cambridge, UK, Cambridge Univ. Press, p. 107–118.

Thiemens, M. H., and Hedenreich, J. E., 1983, The mass independent fractionation of oxygen: A novel isotope effect and its possible cosmochemical implications: Science, v. 219, p. 1073–1075.

Virag, A., Zinner, E., Amari, S., and Anders, E., 1991, An ion microprobe study of corundum in the Murchison meteorite: Implications for ^{26}Al and ^{16}O in the early solar system: Geochim. et Cosmochim. Acta, v. 55, p. 2045–2062.

Völkening, J., and Papanastassiou, D. A. P., 1989, Iron isotope anomalies: Astrophys. Jour. (Lett.), v. 347, p. L43–L46.

_____, 1990, Zinc isotope anomalies: Astrophys. Jour. (Lett.), v. 358, p. L29–L32.

Wasserburg, G. J., 1985, Short-lived nuclei in the early solar system, *in* Black, D. C., and Matthews, M. S., eds., Protostars & planets II: Tucson, Univ. of Arizona Press, p. 703–737.

Wasserburg, G. J., Gallino, R., Busso, M., Goswami, J. N., and Raiteri, C. M., 1995, Injection of freshly synthesized ^{41}Ca in the early solar nebula by an AGB star: Astrophys. Jour. (Lett.), v. 440, p. L101–L104.

Weber, D., and Bischoff, A., 1994, The occurrence of grossite ($CaAl_4O_7$) in chondrites: Geochim. et Cosmochim. Acta, v. 58, p. 3855–3877.

Weber, D., Zinner, E., and Bischoff, A., 1995, Trace element abundances and magnesium, calcium, and titanium isotopic compositions of grossite-containing inclusions from the carbonaceous chondrite Acfer 182: Geochim. et Cosmochim. Acta, v. 59, p. 803–823.

Wiens, R. C., Huss, G. R., and Burnett, D. S., 1999, The solar oxygen-isotopic composition: Predictions and implications for solar nebula processes: Meteorit. Planet. Sci., v. 34, p. 99–107.

Woolum, D. S., and Cassen, P., 1999, Astronomical constraints on nebular temperatures: Implications for planetesimal formation: Meteorit. Planet. Sci., v. 34, p. 897–907.

Young, E. D., and Russell, S. S., 1998, Oxygen reservoirs in the early solar nebula inferred from an Allende CAI: Science, v. 282, p. 452–455.

Zinner, E., 1998, Stellar nucleosynthesis and the isotopic composition of presolar grains from primitive meteorites: Ann. Rev. Earth Planet. Sci., v. 26, p. 147–188.

Zinner, E., Fahey, A., Goswami, J. N., Ireland, T. R., and McKeegan, K. D., 1986, Large ^{48}Ca anomalies are associated with ^{50}Ti anomalies in Murchison and Murray hibonites: Astrophys. Jour. (Lett.), v. 311, p. L103–L107.